arXiv:hep-th/9608035v1 7 Aug 1996

Solving Gauge Field Theory by Discretized Light-Cone Quantization

Hans-Christian Pauli
Max-Planck-Institut für Kernphysik
D-69029 Heidelberg

24 January 1996; revised 31 July 1996

Abstract

The canonical front form Hamiltonian for non-Abelian SU(N) gauge theory in 3+1 dimensions is mapped on an effective Hamiltonian which acts only in the Fock space of one quark and one antiquark. The approach is non-perturbative and exact. It is based on Discretized Light-Cone Quantization and the Method of Iterated Resolvents. The method resums the diagrams of perturbation theory to all orders in the coupling constant and is free of Tamm-Dancoff truncations in the Fock-space. Emphasis is put on dealing accurately with the many-body aspects of gauge field theory. Pending future renormalization group analysis the running coupling is derived to all orders in the bare coupling constant. — The derived effective interaction has an amazingly simple structure and is gauge invariant and frame independent. It is solvable on a small computer like a work station. The many-body amplitudes can be retrieved self-consistently from these solutions, by quadratures without solving another eigenvalue problem. The structures found allow also for developing simple phenomenological models consistent with non-Abelian gauge field theory.

Preprint MPIH-V25-1996

Contents

1 Introduction and Motivation

One of the most important tasks in hadron physics is to calculate and understand the mass spectrum and the wave functions of physical hadrons from a covariant quantum field theory. The wave functions encode all the properties which are needed for a phenomenological description of experiments. Wave functions and probability amplitudes have a natural appearance in a Hamiltonian approach.

But the Hamiltonian bound state problem is notoriously difficult in a field theory. Procedures like those of Schwinger and Dyson or of Bethe and Salpeter are not easy to cope with in practice as reviewed recently in [1]. Actually, the difficulties were considered so enormous that the Hamiltonian approach was given up in the Fifties alltogether in favor of Feynman's action oriented approach. Modern successors like the Lattice Gauge Theories [2, 3] govern the scene, maturing from infancy in recent times [4]. Phenomenological models [5, 6, 7, 8] are closer to experiment and have the different objective to classify the bulk of empirical data. They leave little doubt that a heavy meson contains primarily a pair of constituent quarks and *not* an infinity of sea particles as suggested by the perturbative treatment of quantum field theory.

How can one reconcile these models particularly the constituent quark model (CQM) with the quantum field theory of chromodynamics (QCD)? There are several reasons why the front form [9] of Hamiltonian dynamics [10] is one of the very few candidates, see [11, 12, 13] or [14]. Particularly the simple vacuum and the simple boost properties [13, 15, 16, 17] confront with the 'complicated vacuum' and the 'dynamical boosts' of the conventional approach, the instant form. These aspects are stressed also in the arguments of Wilson [18] and collaborators [19]. Nowadays we know that even the front form vacuum is not simple [20, 21, 22], but still *simplier* than in the instant form: The problem can at least be formulated [23, 24].

The success of discretized light-done quantization (DLCQ) particularly in 1+1 dimensions has stirred hope that its apparent simplicities carry over to the physical 3+1 dimensions [25, 27, 26, 28]. But this meets problems, among them: The Hamiltonian matrix increases exponentially fast with the particle number of the Fock states and with the number of transversal momenta. Truncating the Fock space to 2 particles like Tamm [29] and Dancoff [30] invokes perturbation theory, violates gauge invariance and generates non-integrable singularities. One must resort to *ad hoc* procedures to make things working [26]. Truncating to 3 particles [27, 28], the numerical results are inconclusive as to test an onset of convergence.

Even worse than that: Thus far, it is obscure how *any Hamiltonian* including the one on the light cone could be subjected to a renormalization group analysis. This and the possibly large coupling constant has motivated Wilson [19] to give up the one-to-one connection with canonical field theory and to propose a radically new procedure in which the renormalization properties of front form operators play the crucial role. The problem is a very deep one and appears also in Quantum Electrodynamics (QED). In QED, the smallness of the coupling constant obscures the fact that the simple Coulomb potential between two point charges has not been derived from field theory thus far with other than perturbative methods. Although higher order effects are expected to be small, and are indeed so, see for example [31, 32, 33] and [34], no manifestly non-perturbative and closed analytical procedures are at hand. This is remarkable. In QCD the problems are only accentuated due to the larger coupling constant.

By practical considerations one must reduce the matrix dimension of the Hamiltonian. But the reduction to comparatively small matrices is more than merely a technical issue. It becomes *a matter of principle*. When analyzing the source of the difficulty one realizes that the many-body aspects of a field theory have not been mastered thus far: Precisely those are treated in perturbation theory and precisely those are responsible for the large matrix dimensions. It is here where the present work supposedly contributes. The many-body aspects are kept in the form as they want

to appear, as resolvents, and these *are not expanded* as perturbative series.

Our point is then: One should solve first the many-body aspects of the canonical Hamiltonian, which has not been done thus far, and then think on the problems of renormalization. This is not in conflict with [19], but we emphasize a different aspects of the problem. One is faced then with problems similar to conventional many-body physics, problems as one meets them in the theory of atoms, nuclei or of solids. Remarkably, one can carry out this programme essentially without assumption, and still arrive at a solvable equation. As a matter of fact it is also simple.

At the core of this work is a new method, the 'method of iterated resolvents' to be introduced in section 4. It allows to do 'perturbation theory to all orders' and 'perturbation theory in medium' without a smallness parameter. For to be specific, some of the ingredients of earlier work [13], particularly the Lagrangian and the DLCQ-Fock-space for QCD, are summarized shortly in section 2. Section 3 summarizes the theory of effective interactions as known from the literature [35] and displays why the Tamm-Dancoff approach [29, 30] is bound to fail. The results of section 4 are then applied to QCD in section 5. At the end of many formal manipulations one takes the continuum limit. The effective interaction of a quark and an antiquark will then turn out as a sum of two terms which have an intuitively appealing interpretation: (1) The effective potential U, generated by the exchange of one effective gluon which is absorbed either by the same or by the other quark; and (2) The effective annihilation interaction U_a, where the quark and antiquark annihilate into two effective gluons. The potential U is derived explicitly in section 6, and section 7 summarizes the results including a broader discussion on their possible future application.

2 The front form Hamiltonian for Quantum Chromodynamics

Both in non-relativistic quantum mechanics and in field theory, the Hamiltonian operator propagates the system in time. In a covariant theory the concept of 'time' can be generalized, since the space-time parametrization is arbitrary. But following Dirac [9], there are no more than three standard forms how to choose generalized time and the corresponding Hamiltonian dynamics: the 'instant', the 'front' and the 'point' form. In this section we shall summarize [10, 11, 12, 13] the front form Hamiltonian for QCD, actually for SU(N),

The time-like coordinate is chosen as $x^+ = t+z$, the space-like coordinates as $\vec{x} = (x, y, t-z) \equiv (\vec{x}_\perp, x^-)$. The four-vector of space-time is thus $x^\mu = (x^+, \vec{x}_\perp, x^-)$. In QCD the vector potentials $(\mathbf{A}^\mu)_{cc'}$ are 3×3 matrices, and the Dirac spinors carry a color index c, *i.e.* $\Psi_{\alpha,c}$ with $c = 1, 2, 3$. The Lagrangian density is given by the hermitian operator

$$\mathcal{L} = -\frac{1}{2}\mathrm{Tr}\mathbf{F}^{\mu\nu}\mathbf{F}_{\mu\nu} + \frac{1}{2}\Big[\overline{\Psi}(i\gamma^\mu \mathbf{D}_\mu - m_\mathrm{F})\Psi + \mathrm{h.c.}\Big] \,, \tag{1}$$

expressed in terms of the covariant derivative $\mathbf{D}_\mu \equiv \partial_\mu + ig\mathbf{A}_\mu$ and the color-electromagnetic fields $\mathbf{F}^{\mu\nu} \equiv \partial^\mu \mathbf{A}^\nu - \partial^\nu \mathbf{A}^\mu + ig\,[\mathbf{A}^\mu, \mathbf{A}^\nu]$. The four components of the energy-momentum vector

$$P^\nu = \frac{1}{2}\int_\Omega dx^-\, d^2\vec{x}_\perp \,\Big(2\mathrm{Tr}\mathbf{F}^{+\kappa}\mathbf{F}_\kappa{}^\nu + \frac{1}{2}\Big[\overline{\Psi} i\gamma^+ \mathbf{D}^\nu \Psi + \mathrm{h.c.}\Big] - g^{+\nu}\mathcal{L}\,\Big) \,, \tag{2}$$

i.e. $P^\nu = (P^+, \vec{P}_\perp, P^-)$, are strict constants of the motion. Its space-like components $\vec{P}_\perp = (P^1, P^2)$ and P^+ do not depend on the interaction and in momentum representation are diagonal operators. The time-like component $P^- = 2P_+$ depends on the interaction and propagates the system in the light-cone time x^+, *i.e.* $i\frac{\partial}{\partial x^+}|\Psi\rangle = P_+|\Psi\rangle$, and therefore is the proper front form Hamiltonian [13]. The contraction of these four operators

$$P^\mu P_\mu = P^+P^- - \vec{P}_\perp^{\,2} \qquad \equiv H_\mathrm{LC} \equiv H \tag{3}$$

is Lorentz *invariant* and refered to somewhat improperly but conveniently as the 'light-cone Hamiltonian $H_{\rm LC}$' [13], or shortly H. One seeks a representation in which H is diagonal,

$$H|\Psi_i\rangle = E_i|\Psi_i\rangle \ . \tag{4}$$

Note that the eigenvalues E_i and matrix elements of H somewhat unusually carry the dimension of an invariant-mass-squared.

Periodic boundary conditions on $\mathcal{L}$ can be realized by periodic boundary conditions on the vector potentials $\mathbf{A}^\mu$ and anti-periodic boundary conditions on the spinor fields Ψ_α because $\mathcal{L}$ is bilinear in the latter. One expands these fields into plane wave states and satifies the boundary conditions by *discretizing* the momenta, hence Discretized Light-Cone Quantization (DLCQ), *i.e.*

$$\begin{aligned} p_- &= \begin{cases} \frac{\pi}{L}n, & \text{with } n = \frac{1}{2}, \frac{3}{2}, \ldots, \infty \ \text{ for fermion fields,} \\ \frac{\pi}{L}n, & \text{with } n = 1, 2, \ldots, \infty \ \text{ for boson fields,} \end{cases} \\ \text{and} \quad \vec{p}_\perp &= \frac{\pi}{L_\perp}\vec{n}_\perp, \quad \text{with } n_x, n_y = 0, \pm 1, \pm 2, \ldots, \pm\infty \quad \text{for both .} \end{aligned} \tag{5}$$

This is done at the expense of introducing two length parameters, L and $L_\perp$, which define a normalization volume $\Omega \equiv 2L(2L_\perp)^2$. More explicitly, the free fields are expanded as Fourier sums

$$\begin{aligned} \widetilde{\Psi}_\alpha(x) &= \frac{1}{\sqrt{\Omega}} \sum_q \frac{1}{\sqrt{p^+}} \left(b_q u_\alpha(p,\lambda) e^{-ipx} + d_q^\dagger v_\alpha(p,\lambda) e^{ipx} \right), \\ \text{and} \quad \widetilde{A}_\mu(x) &= \frac{1}{\sqrt{\Omega}} \sum_q \frac{1}{\sqrt{p^+}} \left(a_q \epsilon_\mu(p,\lambda) e^{-ipx} + a_q^\dagger \epsilon_\mu^\star(p,\lambda) e^{ipx} \right) \ , \end{aligned} \tag{6}$$

particularly for the two transversal vector potentials $\widetilde{A}^i \equiv \widetilde{A}^i_\perp$, $(i = 1, 2)$. Each particle is on its mass-shell $p^\mu p_\mu = m^2$. Its four-momentum is $p^\mu = (p^+, \vec{p}_\perp, p^-)$ with $p^- = (m^2 + \vec{p}_\perp^{\,2})/p^+$. Each particle state "$q$" is then characterized by six quantum numbers:

$$q = (n, n_x, n_y, \lambda, c, f) = (p^+, \vec{p}_\perp, \lambda, c, f) = (x, \vec{p}_\perp, \lambda, c, f) \ . \tag{7}$$

The first three, (n, n_x, n_y), specify the space-like momentum and λ the helicity $\uparrow$ or $\downarrow$. A quark is specified further by color c and flavor f. Gluons carry no flavour, and the color index c is substituted by the glue index a. The creation and destruction operators like $a_q^\dagger$ and a_q create and destroy single particle states q, respectively, and obey the usual (anti-) commutation relations like

$$[a_q, a_{q'}^\dagger] = \{b_q, b_{q'}^\dagger\} = \{d_q, d_{q'}^\dagger\} = \ \delta_{q,q'} \ . \tag{8}$$

As an advantage of DLCQ, all quantum numbers are discrete. One deals thus only with simple (and dimensionless) Kronecker symbols. The spinors u_α and v_α and the transversal polarization vectors $\vec{\epsilon}_\perp$ are the usual ones [10] and defined in [13].

A thorough treatment should include the zero modes of the gauge fields particularly those of A^+. Their importance had been demonstrated [23, 24] for the vacuum sector. Here one deals with the particle sectors and their massive excitations. Explicit calculations with [36] and without them [37] yield however the same results in the continuum limit. The global and the gauge zero modes [23, 24] are therefore discarded in the sequel, and the usual light-cone gauge [10, 13] $\mathbf{A}^+ = 0$ is used. The light-cone Gauss equation, *i.e.* $\partial_\mu F_a^{\mu.+} = g J_a^+$, see [13] and [24], and the expansions in Eq.(6) complete the specification of all vector potentials $\mathbf{A}^\mu$. The space-like integrations in Eq.(2) can be carried out explicitly, leading essentially to Kronecker deltas. One ends up with the light-cone energy-momenta [13] as operators acting in Fock space, *i.e.* $P^\nu = P^\nu(a_q, a_q^\dagger, b_q, b_q^\dagger, d_q, d_q^\dagger)$. The various terms in the Hamiltonian are conveniently classified by a sum of four terms [13], *i.e.*

$$H = T + V + F + S \ . \tag{9}$$

The kinetic energy T survives the limit of the coupling constant g going to zero. Since it is diagonal in Fock-space representation, its eigenvalue is the *free invariant mass squared* of the particular Fock state. The *vertex interaction* V is the relativistic interaction *per se*. It is linear in g and changes the particle number by 1 and *only by* 1. Matrix elements of V which change the particle number by 3 (as in the instant form) are strictly zero in DLCQ: The vacuum *does not fluctuate*. The instantaneous interactions F and S are gauge artefacts, are consequences of working in the light-cone gauge and proportional to g^2. The seagull interaction S conserves the particle number. The fork interaction F changes the particle number *only* by 2. As illustrated below in Figure 1, each block in the Hamiltonian matrix is therefore either the zero matrix, or has *only* seagull-, or *only* vertex-, or *only* fork-interactions, with very simple matrix elements tabulated in [13].

There is *one and only one* reference state which is annihilated by all destruction operators, namely the *Fock-space vacuum* $|vac\rangle$. Therefore, the Hilbert space for the single-particle creation and annihilation operators is the Fock space. It is the complete set of all possible states

$$|\Phi_i\rangle = N_i \; b^\dagger_{q_1} b^\dagger_{q_2} \ldots b^\dagger_{q_N} \; d^\dagger_{q_1} d^\dagger_{q_2} \ldots d^\dagger_{q_{\bar{N}}} \; a^\dagger_{q_1} a^\dagger_{q_2} \ldots a^\dagger_{q_{\widetilde{N}}} |vac\rangle \; , \tag{10}$$

subject to be eigenfunctions of the space-like momenta, with *fixed eigenvalues* P^+ and $\vec{P}_\perp$, *i.e.*

$$P^+ = \sum_\nu p^+_\nu = \frac{2\pi}{L} K \; , \quad \text{and} \quad \vec{P}_\perp = \sum_\nu (\vec{p}_\perp)_\nu \; . \tag{11}$$

The sums run over all particles in a Fock state. As consequence of discretization, the Fock states are denumerable and orthonormal: $\langle \Phi_i | \Phi_j \rangle = \delta_{ij}$. As usual, the *momentum fraction* carried by the particle is denoted by $x = p^+/P^+$, and the sum of all fractions is constrained to $\sum_\nu x_\nu = 1$. Note that the Fock states can be made color neutral. Since P^+ has only positive eigenvalues and since each particle has a lowest possible value of p^+, the number of particles in a Fock state is limited for any fixed value of the *harmonic resolution* K [15, 16]. Next to the simple vacuum, this is another pecularity of DLCQ.

For to enumerate all possible Fock states for a meson with a fixed harmonic resolution, one needs a classification scheme. A possible one is displayed in Figure 1. With Fock states being color-singlets, the lowest possible value one can have for K is $K = 1$. This allows for one $q\bar{q}$-pair, at the most. For $K = 2$, the Fock space contains in addition the $g\,g$- and the $q\bar{q}\,g$-sectors. For $K = 4$, one has at most 8 particles, namely 4 $q\bar{q}$-pairs. In the figure all 13 Fock-space sectors possible for K up to 4 are denumerated by $n = 1, \ldots, 13$. Note that the classification of these sectors does not change when K is increased: one just adds more complicated Fock space sectors to the figure. The number of sectors grows quadratically with K and has the value $N_K = (K+1)(K+2)/2 - 2$.

In analogy to the figure, one can rewrite Eq.(4) as a *block matrix equation*:

$$\sum_{m=1}^{N_K} \langle n|H|m\rangle \; \langle m|\Psi_i\rangle = E_i \; \langle n|\Psi_i\rangle \qquad \text{for all } n = 1, 2, \ldots, N_K \; . \tag{12}$$

The numbers n (m) denumerate the sectors. The problem is solved if one can find the sector wave functions $\langle n|\Psi_i\rangle$ for one or several eigenstates Ψ_i. Note that each sector contains many individual Fock states with different values of x, $\vec{p}_\perp$ and λ.

Actually, right from the beginning one could have chosen the conventional procedure. One could have written Eq.(12) in the *continuum limit*, replacing sums by integrals according to

$$\sum_{p^+=\frac{\pi}{2L}}^{P^+} \sum_{\vec{p}_\perp} \longrightarrow \frac{P^+}{2} \, \frac{\Omega}{(2\pi)^3} \int_0^1 dx \int d^2\vec{p}_\perp \; . \tag{13}$$

Figure 1: *The Hamiltonian matrix for a SU(N)-meson. The matrix elements are represented by the letters S, V, and F, corresponding to seagull, vertex, and fork-interactions, respectively. For better orientation, the diagonal blocs are marked by ($\bullet$) and the zero matrices by ($\cdot$). (In the preprint this table is replaced by a figure with the diagrams.)*

K	N_p	Sector	N_p n	2 1	2 2	3 3	4 4	3 5	4 6	5 7	6 8	4 9	5 10	6 11	7 12	8 13
1	2	$q\bar{q}$	1	$\bullet$	S	V	F	$\cdot$	F	$\cdot$	$\cdot$	$\cdot$	$\cdot$	$\cdot$	$\cdot$	$\cdot$
2	2	$g\ g$	2	S	$\bullet$	V	$\cdot$	V	F	$\cdot$	$\cdot$	F	$\cdot$	$\cdot$	$\cdot$	$\cdot$
2	3	$q\bar{q}\ g$	3	V	V	$\bullet$	V	S	V	F	$\cdot$	$\cdot$	F	$\cdot$	$\cdot$	$\cdot$
2	4	$q\bar{q}\,q\bar{q}$	4	F	$\cdot$	V	$\bullet$	$\cdot$	S	V	F	$\cdot$	$\cdot$	F	$\cdot$	$\cdot$
3	3	$g\ g\ g$	5	$\cdot$	V	S	$\cdot$	$\bullet$	V	$\cdot$	$\cdot$	V	F	$\cdot$	$\cdot$	$\cdot$
3	4	$q\bar{q}\ g\ g$	6	F	F	V	S	V	$\bullet$	V	$\cdot$	S	V	F	$\cdot$	$\cdot$
3	5	$q\bar{q}\,q\bar{q}\ g$	7	$\cdot$	$\cdot$	F	V	$\cdot$	V	$\bullet$	V	$\cdot$	S	V	F	$\cdot$
3	6	$q\bar{q}\,q\bar{q}\,q\bar{q}$	8	$\cdot$	$\cdot$	$\cdot$	F	$\cdot$	$\cdot$	V	$\bullet$	$\cdot$	$\cdot$	S	V	F
4	4	$g\ g\ g\ g$	9	$\cdot$	F	$\cdot$	$\cdot$	V	S	$\cdot$	$\cdot$	$\bullet$	V	$\cdot$	$\cdot$	$\cdot$
4	5	$q\bar{q}\ g\ g\ g$	10	$\cdot$	$\cdot$	F	$\cdot$	F	V	S	$\cdot$	V	$\bullet$	V	$\cdot$	$\cdot$
4	6	$q\bar{q}\,q\bar{q}\ g\ g$	11	$\cdot$	$\cdot$	$\cdot$	F	$\cdot$	F	V	S	$\cdot$	V	$\bullet$	V	$\cdot$
4	7	$q\bar{q}\,q\bar{q}\,q\bar{q}\ g$	12	$\cdot$	$\cdot$	$\cdot$	$\cdot$	$\cdot$	$\cdot$	F	V	$\cdot$	$\cdot$	V	$\bullet$	V
4	8	$q\bar{q}\,q\bar{q}\,q\bar{q}\,q\bar{q}$	13	$\cdot$	$\cdot$	$\cdot$	$\cdot$	$\cdot$	$\cdot$	$\cdot$	F	$\cdot$	$\cdot$	$\cdot$	V	$\bullet$

But apart from introducing innumerable integration variables and separate summation indices like color, flavor and spin, one tends to loose oversight in a set of coupled integral equations as implied by Eq.(12). Since there is nothing wrong about thinking like Dirac in terms of matrices, we continue to do so because we find it more convenient.

Each sector with a given parton number has arbitrarily many Fock states whose transversal momenta add up to a given value of $\vec{P}_\perp$. One needs a cut-off. Following Lepage and Brodsky [10, 11, 12] the Fock space is regulated by the condition that the free invariant mass shall not exceed a limit, *i.e.*

$$\sum_\nu \left(\frac{m^2+\vec{p}_\perp^{\,2}}{x}\right)_\nu \leq \quad \Lambda_n^2 \quad + \quad \left(\sum_\nu m_\nu\right)^2 . \tag{14}$$

The sector dependent mass scales Λ_n will not be needed below. They govern how much the particles can go off their equilibrium values $\vec{\overline{p}}_\perp = \vec{0}$ and $\overline{x}_\nu = m_\nu / \sum_\nu m_\nu$. The number of individual Fock states in DLCQ is thus finite, and the Hamiltonian matrix will have a finite dimension. A finite matrix can be diagonalized numerically.

This – in a nutshell – is the programme of Discretized Light-Cone Quantization [15]. One tends to conclude that the solution of the bound-state problem for a gauge field theory like QCD is solvable on a computer.

3 The Effective Interaction and the Tamm-Dancoff Approach

DLCQ applied to gauge theory faces a formidable matrix diagonalization problem. The problem is even worse than in non-relativistic many-body theory. Here are the steps one should take in principle: In a first step one sets up the Fock space as discussed in the previous section. In a second step one calculates the finite dimensional Hamiltonian matrix as illustrated in Figure 1. In

a third step one diagonalizes the matrix numerically. Here is the bottleneck of the method: Sooner or later, the matrix dimension exceeds imagination, and other than in 1+1 dimensions one has to develop new tools by matter of principle.

Intuitively one aims at something like an effective interaction between a quark and an antiquark, similar to the effective interaction between a negative and a positive point charge. Effective interactions are a well known tool in many-body physics [35]. To the community the method is known as the Tamm-Dancoff-Approach, as applied first to Yukawa theory for describing the nucleon-nucleon interaction [29, 30]. A look on its salient features is worth the effort.

Consider a Hamiltonian matrix as in Eq.(12) subject to diagonalization, $H|\Psi\rangle = E|\Psi\rangle$. The matrix dimension be N. Explicitly written out, the eigenvalue equation reads

$$\sum_{j=1}^{N} \langle i|H|j\rangle\langle j|\Psi\rangle = E\ \langle i|\Psi\rangle\ , \qquad \text{for } i = 1, 2, \ldots, N. \tag{15}$$

The rows and columns of the matrix can always be split into two parts. One speaks of the P-space $P = \sum_{j=1}^{n} |j\rangle\langle j|$ with $1 < n < N$, and of the rest, the Q-space $Q \equiv 1 - P$. Eq.(15) can then be rewritten conveniently in terms of *block matrices* like

$$\begin{pmatrix} \langle P|H|P\rangle & \langle P|H|Q\rangle \\ \langle Q|H|P\rangle & \langle Q|H|Q\rangle \end{pmatrix} \begin{pmatrix} \langle P|\Psi\rangle \\ \langle Q|\Psi\rangle \end{pmatrix} = E\ \begin{pmatrix} \langle P|\Psi\rangle \\ \langle Q|\Psi\rangle \end{pmatrix}\ , \tag{16}$$

or explicitly

$$\langle P|H|P\rangle\ \langle P|\Psi\rangle + \langle P|H|Q\rangle\ \langle Q|\Psi\rangle \;=\; E\,\langle P|\Psi\rangle\ , \tag{17}$$

$$\text{and} \qquad \langle Q|H|P\rangle\ \langle P|\Psi\rangle + \langle Q|H|Q\rangle\ \langle Q|\Psi\rangle \;=\; E\,\langle Q|\Psi\rangle\ . \tag{18}$$

Rewrite the second equation as

$$\langle Q|E - H|Q\rangle\ \langle Q|\Psi\rangle = \langle Q|H|P\rangle\ \langle P|\Psi\rangle, \tag{19}$$

and observe that the quadratic matrix $\langle Q|E - H|Q\rangle$ could be inverted to express the Q-space wavefunction $\langle Q|\Psi\rangle$ in terms of the P-space wavefunction $\langle P|\Psi\rangle$. But here is the problem: The eigenvalue E is unknown at this point. One therefore solves first an other problem: One introduces *the starting point energy* ω as a redundant parameter at disposal, and *defines the resolvent* of the Q-space matrix as the inverse of $\langle Q|\omega - H|Q\rangle$,

$$G_Q(\omega) = \frac{1}{\langle Q|\omega - H|Q\rangle}\ . \tag{20}$$

With Eq.(19) one *defines* then

$$\langle Q|\Psi\rangle \equiv \langle Q|\Psi(\omega)\rangle = G_Q(\omega)\langle Q|H|P\rangle\ \langle P|\Psi\rangle\ . \tag{21}$$

Inserting this into Eq.(17) yields an eigenvalue equation in the P-space

$$\langle P|H_{\rm eff}(\omega)|P\rangle \qquad \langle P|\Psi_k(\omega)\rangle = E_k(\omega)\ \langle P|\Psi_k(\omega)\rangle\ , \qquad \text{with} \tag{22}$$

$$\langle P|H_{\rm eff}(\omega)|P\rangle \;=\; \langle P|H|P\rangle + \langle P|H|Q\rangle\ G_Q(\omega)\ \langle Q|H|P\rangle\ . \tag{23}$$

The effective interaction in the P-space is thus well defined: It is the original matrix $\langle P|H|P\rangle$ plus a part where the system is scattered virtually into the Q-space, propagating there by impact of the true interaction, and finally scattered back into the P-space. Every value of ω defines a different

Hamiltonian and a different spectrum. Varying ω one generates a set of *energy functions* $E_k(\omega)$. Whenever one finds a solution to the *fixpoint equation* [38, 39]

$$E_k(\omega) = \omega, \tag{24}$$

one has found one of the true eigenvalues and eigenfunctions of H, by construction.

One should emphasize that one finds this way *all* N *eigenvalues* of H, see also [38], irrespective of how small one chooses the P-space. Even if one chooses a P-space with 'matrix' dimension $n = 1$, the single energy function $E_1(\omega)$ contains the infomation on *all* eigenvalues: The $N - 1$ poles of $E_1(\omega)$ generate the N eigenvalues by means of Eq.(24). Explicit examples for that can be found in [38, 39] and in Appendix B. It looks as if one has mapped a difficult problem, the diagonalization of a huge matrix onto a simplier problem, the diagonalization of a much smaller matrix. This is true, but not completely. One has to invert a matrix. In practice, the inversion of a matrix is as diffficult as its diagonalization. In addition, one has to vary ω and solve the fixpoint equation (24). The numerical work is thus rather larger than smaller as compared to a direct diagonalization.

The advantage of working with the so defined effective interaction is that resolvents can be approximated systematically. The two resolvents

$$G_Q(\omega) = \frac{1}{\langle Q|\omega - T - U|Q\rangle} \ , \quad \text{and } G_0(\omega) = \frac{1}{\langle Q|\omega - T|Q\rangle} \ , \tag{25}$$

defined once with and once without the non-diagonal interaction in the Hamiltonian $H = T + U$, respectively, are identically related by

$$G_Q(\omega) = G_0(\omega) + G_0(\omega)\ U\ G_Q(\omega) \ , \quad \text{or by} \tag{26}$$

$$G_Q(\omega) = G_0(\omega) + G_0(\omega)UG_0(\omega) + G_0(\omega)UG_0(\omega)UG_0(\omega) + \dots \ , \tag{27}$$

that is, by the *infinite series of perturbation theory*. The point is, of course, that the kinetic energy T is a diagonal matrix which can be trivially inverted to get $G_0(\omega)$.

After these formal considerations we return to gauge theory and its Fock space representations as displayed in Figure 1. The identification of the $q\bar{q}$-space with the P-space and the related effective interaction between one constituent (q) with an other ($\bar{q}$) appears as the most natural thing to do. But now the trouble starts: Like Tamm and Dancoff [29, 30] one truncates the above series to the very first term $H_{\text{eff}} = H + H|Q\rangle\langle Q|(\omega - T)^{-1}|Q\rangle\langle Q|H$. But the Tamm-Dancoff procedure fails for light-cone kinematics: When taken literally, the effective interaction has a non-integrable singularity [26]. Even worse, simple estimates show that the series in Eq.(27) diverges [27] order by order, all that irrespective of violating badly gauge invariance due to the truncation. One has to invent *ad hoc* measures to get things working [26]. One could try to *resum the series* in Eq.(27) at least partially, guided for example, like in Quantum Electrodynamics, by a smallness assumption on the coupling constant. When one tries that, one gets lost soon in the murky depths of perturbation theory *driven to all orders*, and quits the game. One the other hand, the procedure displayed in Eqs.(16) to (26) *is in principle exact*. Maybe one should look at it from an other point of view. One of the many conclusions might be that the interaction term in the denominator of Eq.(25) should be dealt with in a better way, for example, by the 'method of iterated resolvents' to be presented next.

4 The Method of Iterated Resolvents

DLCQ applied to gauge field theory is, as mentioned, particular among matrix diagonalization problems to the extent that a *finite number* of Fock-space sectors like in Figure 1 appears in the

most natural way. The same holds true for quantum-mechanical A-body problems where the Fock space can be classified in terms of the *finite number* of 0-particle-0-hole (0-ph), 1-ph, ..., A-ph sectors, see for example [40]. In either case the block matrix in sparse. Most of the blocks are zero matrices due to the nature of the underlying Hamiltonian. One should make use of that!

In DLCQ one is confronted with the diagonalization of a *finite dimensional block matrix*, for which Eq.(16) represents the example of 2×2 blocks. The step from Eq.(16) to Eq.(22) can then be interpreted as the reduction of a block matrix dimension from 2 to 1. As a matter of fact, if one chooses the Q-space identical with last sector N_K in Figure 1 and the P-space with the rest, $Q = 1 - P$, one reduces the block matrix equation from dimension N_K to $N_K - 1$, with an effective interaction acting in the now smaller space. This procedure can be repeated, and again iterated, until one arrives at an effective interaction of block matrix dimension $n = 1$, *with a well defined* effective interaction in the '1'-space. All that is needed is a reasonable notation [41].

Suppose, in the course of this reduction, one has arrived at block matrix dimension n, with $1 < n < N_K$. Denote the corresponding effective interaction $H_n(\omega)$. The eigenvalue problem corresponding to Eq.(22) reads now

$$\sum_{j=1}^{n} \langle i|H_n(\omega)|j\rangle\langle j|\Psi(\omega)\rangle = E(\omega)\ \langle i|\Psi(\omega)\rangle\ , \qquad \text{for } i = 1, 2, \ldots, n. \tag{28}$$

Observe that i and j refer here to sector numbers. Now, in analogy to Eqs.(20) and (21), define

$$G_n(\omega) \;=\; \frac{1}{\langle n|\omega - H|n\rangle}\ , \qquad \text{and} \tag{29}$$

$$\langle n|\Psi(\omega)\rangle \;=\; G_n(\omega) \sum_{j=1}^{n-1} \langle n|H_n(\omega)|j\rangle\ \langle j|\Psi(\omega)\rangle\ , \tag{30}$$

respectively. The effective interaction in the $(n-1)$-space becomes then [41]

$$H_{n-1}(\omega) = H_n(\omega) + H_n(\omega)G_n(\omega)H_n(\omega) \tag{31}$$

for every block matrix element $\langle i|H_{n-1}(\omega)|j\rangle$. To get the corresponding eigenvalue equation one substitutes n by $n-1$ everywhere in Eq.(28). Everything proceeds like in section 3, including the fixed point equation $E(\omega) = \omega$. But one has achieved much more: Eq.(31) is a *recursion relation* which holds for all $1 < n < N_K$! The only convention one must have, of course, is that one has started from the bare interaction H, thus $H_{N_K} = H$. The rest is algebra and interpretation.

How can the procedure be interpreted? One gets some inspiration from the paradigm of a 4×4 block matrix as explicitly dealt with in Appendix B. The consequences of Eq.(31) are worked out in Appendix C: When expressed in terms of the bare interaction (matrices) H and the resolvents G_n, the effective interaction in sector n wants to develope *chains* like

$$H_n(\omega) = \ldots\ + HG_l(\omega)HG_m(\omega)HG_r(\omega)H + \ \ldots\ , \qquad \text{with } l, m, r > n. \tag{32}$$

The order of the chains is given by the number of propagators and not, as usual, by the power of the coupling constant. The maximum order of the chains *is strictly finite for a finite matrix*, as opposed to the infinite series of perturbation theory. The sector numbers in the chains are not arbitrary, but obey the rules tabulated in Appendix C. For example, the effective interaction H_n has no propagator with sector number n. This implies that the system *can not fall back*, a feature distincly different from the usual perturbative propagators displayed in Eq.(25). Moreover, most of the chains vanish from the outset for the DLCQ-Hamiltonian: It suffices that only one of the four bare block matrix elements appearing in Eq.(32), namely $\langle n|H|l\rangle$, $\langle l|H|m\rangle$, $\langle m|H|r\rangle$, or $\langle r|H|n\rangle$ is

Figure 2: *The Hamiltonian matrix for a SU(N)-meson when only vertex diagrams (V) are included. Compare also with Figure 1. Zero matrices are marked by (·). (In the preprint this table is replaced by a figure with the diagrams.)*

K	N_p	Sector	N_p / n	2 / 1	2 / 2	3 / 3	4 / 4	3 / 5	4 / 6	5 / 7	6 / 8	4 / 9	5 / 10	6 / 11	7 / 12	8 / 13
1	2	$q\bar{q}$	1	•		V		·		·	·	·	·	·	·	·
2	2	$g\ g$	2		•	V	·	V		·	·		·	·	·	·
2	3	$q\bar{q}\ g$	3	V	V	•	V		V		·	·		·	·	·
2	4	$q\bar{q}\,q\bar{q}$	4		·	V	•	·		V		·	·		·	·
3	3	$g\ g\ g$	5	·	V		·	•	V	·	·	V		·	·	·
3	4	$q\bar{q}\ g\ g$	6			V		V	•	V	·		V		·	·
3	5	$q\bar{q}\,q\bar{q}\ g$	7	·	·		V	·	V	•	V	·		V		·
3	6	$q\bar{q}\,q\bar{q}\,q\bar{q}$	8	·	·	·		·	·	V	•	·	·		V	
4	4	$g\ g\ g\ g$	9	·		·	·	V		·	·	•	V	·	·	·
4	5	$q\bar{q}\ g\ g\ g$	10	·	·		·		V		·	V	•	V	·	·
4	6	$q\bar{q}\,q\bar{q}\ g\ g$	11	·	·	·		·		V		·	V	•	V	·
4	7	$q\bar{q}\,q\bar{q}\,q\bar{q}\ g$	12	·	·	·	·	·	·		V	·	·	V	•	V
4	8	$q\bar{q}\,q\bar{q}\,q\bar{q}\,q\bar{q}$	13	·	·	·	·	·	·	·		·	·	·	V	•

a zero-matrix. Unpleasant is to some extent, that one has to deal with 'resolvents of resolvents', or with 'iterated resolvents'. On the other hand, each resolvents represents a resummation of all orders in perturbation theory, and it is this particular aspect which makes them interesting, at least.

5 Application to Quantum Chromodynamics

The method of iterated resolvents is almost ideally suited for dealing with the DLCQ matrix for Quantum Chromodynamics, see Figure 1, and for deriving the effective Hamiltonian in the $q\bar{q}$-space.

In doing so, we actually shall use a trick which will simplify considerations enormously. Practitioners in Light-Cone Time-Ordered Perturbation Theory [10, 11, 13, 25] know that they can omit the instantaneous interactions F and S until *they actually compute* a particular diagram. Then, every intrinsic line in a graph must be combined with the instantaneous partner line associated with the gauge artefacts. Only then, the sum of all time ordered diagrams becomes manifestly identical with gauge-invariant Feynmann scattering amplitudes. There is no exception known to this rule, thus far, in all graphs computed explicitly. In the sequel, this 'gauge trick' [25] is adopted by setting formally to zero all block matrices in Figure 1 which are gauge remnants. One then gets a block matrix structure as displayed in Figure 2. The extreme sparseness of this block matrix will allow us to carry the procedures through to the end. When eventually arriving there, we will check explicitely in Appendix D whether the restitution of the gauge artefacts changes anything in the structure of the solution. The answer will be: 'It doesn't'.

When writing down the chains for the block matrix displayed in Figure 2 according to the rules of the method of iterated resolvents, the effective Hamiltonian in the $q\bar{q}$-space becomes

$$H_1 = T_1 + VG_3V + VG_3VG_2VG_3V\ . \tag{33}$$

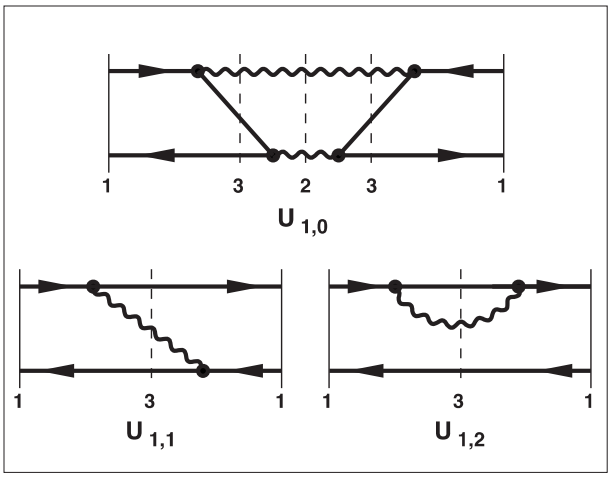

Figure 3: *Three graphs of the effective interaction in the $q\bar{q}$-space. — The lower two graphs correspond to the chain VG_3V, the upper corresponds to $VG_3VG_2VG_3V$. Propagators are represented by vertical dashed lines with a subscript 'n' for the sector.*

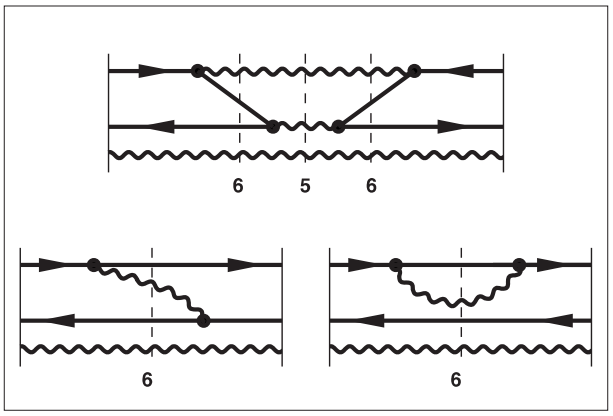

Figure 4: *Graphs of the spectator interaction in the $q\bar{q}\,g$-space. Note the role of the gluon as a spectator.*

Only two chains survive the procedure, one with one, and one with three propagators $G_j = G_j(\omega)$. One checks explicitly with Eqs.(114) and (115) that no chains with four, five or more propagators, are possible, even not for the case of arbitrarily large harmonic resolution K. Eq.(33) stands thus for full QCD in the continuum limit. The gauge trick is thus a great help: Including the gauge artefacts, the effective Hamiltonian in the $q\bar{q}$-space would given 32 non-trivial chains up to order 4. These are explicitly tabulated in Appendix C.

Why are there only two chains in Eq.(33)? The system can scatter out of the $q\bar{q}$-space into the $q\bar{q}\,g$-space by emitting a gluon from the quark or from the antiquark. There is no other way since all other block matrix elements $\langle 1|H|j\rangle$ vanish according to Figure 2. This kills all possible chains which do not start like $VG_3VG_jVG_l\ldots$. The scattering from the $q\bar{q}\,g$-space proceeds either by scattering back to the $q\bar{q}$-space, which is the first chain in Eq.(33), or by scattering into another space by a sequence like G_3VG_j. The rules of MIR require $3 > j > 1$. The only solution $j = 2$ gives the second chain.

What do the chains in Eq.(33) mean in terms of physics? We find it convenient to illustrate that by the diagrams in Figure 3. The first term in the effective Hamiltonian H_1 refering to the kinetic energy (T_1) in the $q\bar{q}$-space needs no illustration. In the second term (VG_3V) the vertex interaction V creates a gluon and scatters the system from the $q\bar{q}(1)$-sector into the $q\bar{q}\,g$-space. As indicated by the vertical line with the subscript '3', the three particles propagate there in '3'-space under impact of the full interaction before the gluon is annihilated. The gluon can be absorbed either by the antiquark or by the quark, corresponding to the two 'interactions' $U_{1,1}$ and $U_{1,2}$, respectively, in the figure. Two further graphs, describing the irradiation of the gluon by the antiquark, are not shown; like throughout in the sequel we use the graphs for the purpose of illustration rather then of a complete description. As the inverse of the non-diagonal Hamiltonian $H_3(\omega)$, the propagator $G_3(\omega)$ is non-diagonal as well, in general. Therefore, despite the total (space-like) momenta being conserved strictly by the interaction and thus by propagation, the space-like momenta of the individual particles can change. A finite size box instead of a thin line would thus be more appropriate for graphically representing propagators. With this proviso in mind, and

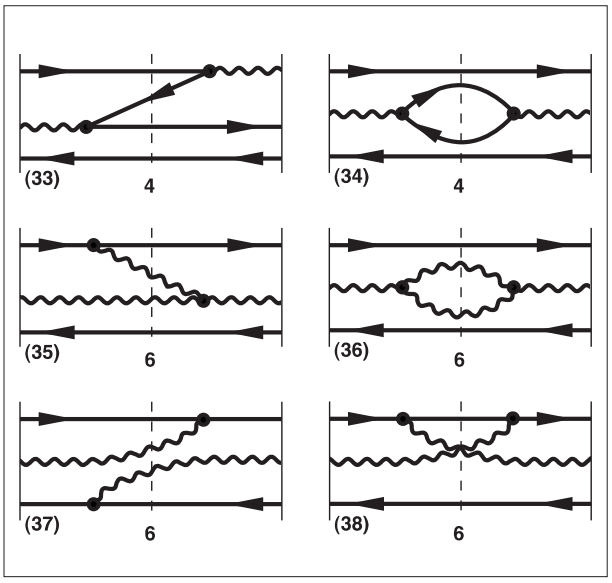

Figure 5: *Six graphs of the participant interaction in the $q\bar{q}\,g$-space.*

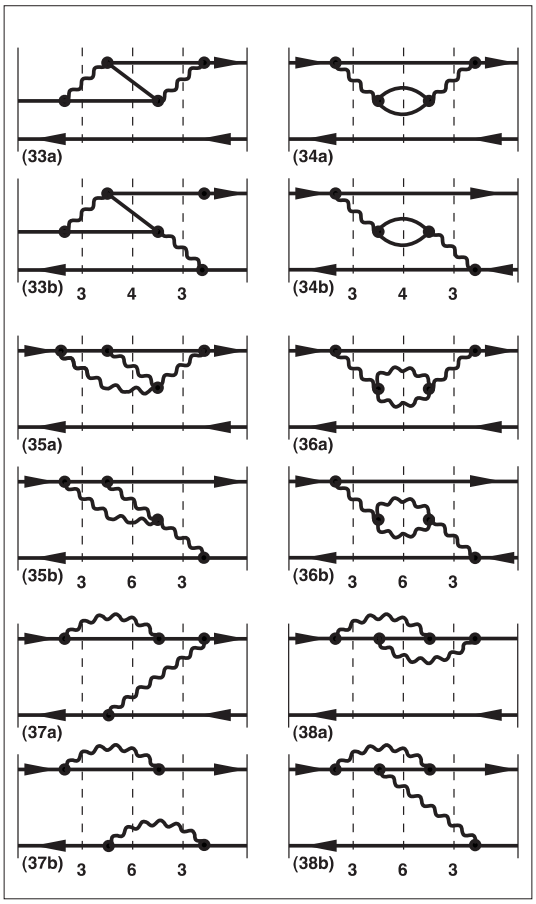

Figure 6: *Twelve graphs corresponding to Fig. 5 with the gluons absorbed after propagation.*

the recognition that an interaction can have several graphs, we proceed. The last term, finally, in Eq.(33) is represented correspondingly by the graph $U_{1,0}$ in Figure 3.

5.1 The quark-pair-glue propagators, and propagation 'in medium'

The mind trained by perturbation theory wonders about all those zillions of graphs, he is used to work with. The answer is that they have neither been ommitted nor neclected but that they reside in the propagators G_i, very effectively 'resumed to all orders'. How do they look?

By the rules established in Appendix C, one obtains consecutively for the effective Hamiltonians in the sectors with one $q\bar{q}$-pair and 1,2,3 or more gluons

$$H_3 = T_3 + VG_6V + VG_6VG_5VG_6V + VG_4V \ , \tag{34}$$

$$H_6 = T_6 + VG_{10}V + VG_{10}VG_9VG_{10}V + VG_7V \ , \tag{35}$$

$$H_{10} = T_{10} + VG_{15}V + VG_{15}VG_{14}VG_{15}V + VG_{11}V \ , \tag{36}$$

respectively, to whose resolvents we refer collectively as the quark-pair-glue propagators. Note that these are all exact relations, by the same reasons as discussed above, for the $q\bar{q}(1)$-sector. Note also that they all have the same structure. They differ from the effective Hamiltonian in the $q\bar{q}$-space, Eq.(33), only by their respective last term, in which a gluon is annihilated into a $q\bar{q}$-pair. Since the

$q\bar{q}$-sector has no gluon, by definition, the corresponding term must be absent there. In passing, one notes the 'replica-structure' of these Hamiltonians and propagators. Like in Russian puppets one has propagators of propagators, and a certain amount of self-similarity cannot be denied. These strucures seem to be particular to gauge theory, abelian or not.

Let us have a look at the diagrammatic representation of these Hamiltonians, and in particular on the effective Hamiltonian in the $q\bar{q}\,g(3)$-sector, Eq.(34). A typical collection is given in Figures 4 and 5. The subset of graphs displayed in Figure 4 looks exactly like the effective interaction in Figure 3, except of the additional gluon. The gluon does not change quantum numbers under impact of the interaction, and acts like a spectator. We thus refer to the graphs in Figure 4 as the 'spectator interaction' $\overline{U}_3$. In the graphs of Figure 5, the gluon undergoes scatterings which correspondingly are refered to as the 'participant interaction' $\widetilde{U}_3$, in the sequel. The effective Hamiltonians the quark-pair-glue sectors $q\bar{q}\,g\ldots g$, as given in Eqs.(34) to (36), can thus be written

$$H_n = T_n + \overline{U}_n + \widetilde{U}_n \ , \quad \text{for} \quad n = 3, 6, 10, 15, \ldots \ , \tag{37}$$

collectively, and with the obvious corresponding definitions.

In terms of physics, the separation into spectators and participants becomes more transparent in a perturbative consideration. Think of the incoming gluon in Figure 5 as being irradiated by a quark, and of the outgoing gluon as to be absorbed either by the quark (a) or by the antiquark (b), and draw the corresponding diagrams. Each diagram in Figure 5 will then be associated with two diagrams in Figure 6. The labels on the diagrams in the figures have no other purpose in the present context than to help the reader with this association. The diagrams in Figure 6 look familiar. Would one do plain perturbation theory, they would be diagrams of order 4 in the coupling constant. Indeed, they look like the familiar mass, vertex or vacuum 'corrections', which are associated usually with the *running coupling constant* [45, 46]. Here, however, we continue to deal with propagators in medium and take the analogue only as an argument why the separation into 'spectators' and 'participants' might be useful.

The essence is that the propagators $\overline{G}_n$ associated with the spectator interaction $\overline{U}_n$, *i.e.*

$$\overline{G}_n = \frac{1}{\omega - T_n - \overline{U}_n} \ , \qquad \left(\text{while } G_n = \frac{1}{\omega - T_n - \overline{U}_n - \widetilde{U}_n} \equiv \frac{1}{\omega - H_n} \right) , \tag{38}$$

are identically related to the full propagators G_n by

$$G_n = \overline{G}_n + \overline{G}_n \, \widetilde{U}_n \, G_n \ . \tag{39}$$

As usual, they can be written as an infinite series

$$G_n = \overline{G}_n + \overline{G}_n \widetilde{U}_n \, \overline{G}_n + \overline{G}_n \widetilde{U}_n \, \overline{G}_n \widetilde{U}_n \, \overline{G}_n + \ldots \ . \tag{40}$$

The main difference to the usual series like in Eq.(26) is, that there the 'unperturbed propagator' $G_0(\omega)$ refers to the system without interactions while here the 'unperturbed propagators' $\overline{G}_n$ contain the interaction in the well defined form of $\overline{U}_n$. One therefore deals here with 'perturbation theory in medium'. Note that the present series is different from the above Eq.(26) also with respect to the physics: The system stays in sector n. This allows for an identical rearrangement of the series

$$G_n = \left[1 + \frac{1}{2} \overline{G}_n \widetilde{U}_n + \frac{3}{8} \overline{G}_n \widetilde{U}_n \, \overline{G}_n \widetilde{U}_n + \ldots \right] \overline{G}_n \left[1 + \frac{1}{2} \widetilde{U}_n \, \overline{G}_n + \frac{3}{8} \widetilde{U}_n \, \overline{G}_n \widetilde{U}_n \, \overline{G}_n + \ldots \right] \ , \tag{41}$$

which can be verified order by order and which, to our recollection, has not been given before. The series in the square bracket are known to be the inverse square, *i.e.*

$$R_n = \frac{1}{\sqrt{1 - \overline{G}_n \widetilde{U}_n}} = 1 + \frac{1}{2} \overline{G}_n \widetilde{U}_n + \frac{3}{8} \overline{G}_n \widetilde{U}_n \, \overline{G}_n \widetilde{U}_n + \ldots \ , \tag{42}$$

and therefore the full propagators can be rewritten identically as

$$G_n = R_n^\dagger \overline{G}_n R_n = \frac{1}{\sqrt{1-\widetilde{U}_n\overline{G}_n}}\,\overline{G}_n\,\frac{1}{\sqrt{1-\overline{G}_n\widetilde{U}_n}}\ . \tag{43}$$

This result can be verified also by closed operator relations. First, one notes the strict identity

$$(1-\widetilde{U}_n\overline{G}_n)(\omega-\overline{H}_n) = \left(1-\widetilde{U}_n\frac{1}{\omega-\overline{H}_n}\right)(\omega-\overline{H}_n) = \omega - H_n\ . \tag{44}$$

Since its adjoint is also correct, one gets

$$G_n^\dagger G_n = \frac{1}{1-U_n\overline{G}_n}\,\frac{1}{(\omega-H_n)^2}\,\frac{1}{1-\overline{G}_n U_n}\ . \tag{45}$$

This is a positive valued operator. Taking the square root with this precaution, gives Eq.(43) as an identity. One thus can proceed without having to worry on the square roots, their ambiguities of signs, and on the convergence of the series. The square matrix R will always be sandwiched between a quark-pair-glue propagator $\overline{G}$ and two vertex interactions V, for which reason it is convenient to introduce $\overline{V}$ as an abbreviation, defined by

$$V\,G_n(\omega)\,V = V\,R_n^\dagger(\omega)\overline{G}_n(\omega)R_n(\omega)\,V \equiv \overline{V}\,\overline{G}_n\,\overline{V}\ . \tag{46}$$

Below, a very natural and physical interpretation is given to the operator R, as being related to 'running coupling constant', but here we continue to proceed formally. We use the above findings to systematically rewrite Eqs.(33)-(36). Working upwards in the hierarchy, one gets consecutively:

$$\overline{H}_6 = T_6 + \overline{V}\,\overline{G}_{10}\overline{V} + \overline{V}\,\overline{G}_{10}\overline{V}G_9\overline{V}\,\overline{G}_{10}\overline{V}\ , \tag{47}$$

$$\overline{H}_3 = T_3 + \overline{V}\,\overline{G}_6\overline{V} + \overline{V}\,\overline{G}_6\overline{V}G_5\overline{V}\,\overline{G}_6\overline{V}\ , \tag{48}$$

$$H_1 = \overline{H}_1 = T_1 + \overline{V}\,\overline{G}_3\overline{V} + \overline{V}\,\overline{G}_3\overline{V}G_2\overline{V}\,\overline{G}_3\overline{V}\ . \tag{49}$$

Instead of being similar, the sector Hamiltonians $\overline{H}_n = T_n + \overline{U}_n$ become equal for suffiently large K. All what is different is that they act in different quark-pair-glue spaces, namely in the $q\bar{q}$-spaces with 1, 2 or more gluons.

The gluons, however, by construction do not take part in the interaction. They act like inert spectators, very much like displayed already in Figures 3 and 4 for the interactions in the $q\bar{q}(1)$- and the $q\bar{q}\,g$-space, respectively. All what one has to do is to update the figures and to replace *each point-like vertex* by say a square, which should symbolize the impact of the operator R.

5.2 The key point: The quark-pair-glue resolvents 'in the solution'

The operators $\overline{H}_n = \overline{H}_n(\omega)$ are *bona fide* Hamiltonians which can be diagonalized on their own

$$\overline{H}_n(\omega)|\Psi_n(\omega)\rangle = E_n(\omega)|\Psi_n(\omega)\rangle\ , \quad \text{for} \quad n = 1,3,6,10,\dots\ . \tag{50}$$

Since the (spectator) gluons do not interact with the bound $q\bar{q}$ system, by construction, one can relate the various spectra, knowing nothing on $\overline{U}_n$ except that the same potential acts only between the quarks. For $n=1$, the Fock states are $|q;\bar{q}\rangle = b_q^\dagger d_{\bar{q}}^\dagger|vac\rangle$ and the eigenvalue equation reads

$$\sum_{q',\bar{q}'}\langle q;\bar{q}|H_1(\omega)|q';\bar{q}'\rangle\langle q';\bar{q}'|\Psi_b(\omega)\rangle = M_b^2(\omega)\langle q;\bar{q}|\Psi_b(\omega)\rangle\ . \tag{51}$$

The eigenstates labeled by b form a complete set of states and denumerate the physical mesons and their spectrum. They correspond to physical particles up to the fact that their invariant mass

$M_b = M_b(\omega)$ still depends on the starting point energy. Correspondingly for $n = 3$, one has $|q;\bar{q};g\rangle = b_q^\dagger d_{\bar{q}}^\dagger a_g^\dagger |vac\rangle$ and

$$\sum_{q',\bar{q}',g'} \langle q;\bar{q};g|\overline{H}_3(\omega)|q';\bar{q}';g'\rangle\langle q';\bar{q}';g'|\psi_{b,s}(\omega)\rangle = M_{b,s}^2(\omega)\langle q;\bar{q};g|\psi_{b,s}(\omega)\rangle \ . \tag{52}$$

Because the gluon is a *non-interacting spectator*, the eigenfunction is a product state $|\psi_{b,s}(\omega)\rangle = |\Psi_b(\omega)\rangle \otimes |\varphi_s\rangle$, labeled by the *two indices* b and s. In fact, the eigenvalues in this sector *must be*

$$M_{b,s}^2 = \frac{M_b^2 + \vec{k}_{g_\perp}^2}{(1-x_g)} + \frac{\vec{k}_{g_\perp}^2}{x_g} \ , \tag{53}$$

corresponding to the free gluon moving with momentum (fraction) $\vec{k}_{g_\perp}$ (x_g) relative to the meson with mass M_b and momentum (fraction) $\vec{k}_{b_\perp} = -\vec{k}_{g_\perp}$ $(x_b = 1 - x_g)$. Correspondingly the eigenvalue in the $q\bar{q}\,g\ldots g$ sectors are

$$M_{b,g\ldots g}^2 = \frac{M_b^2 + \vec{k}_{g_\perp}^2}{(1-x_g)} + \frac{\mu_{g\ldots g}^2 + \vec{k}_{g_\perp}^2}{x_g} \ . \tag{54}$$

Here the meson moves against the cluster of free gluons with free invariant mass $\mu_{g\ldots g}$. Note that these statements are *frame independent* and a direct consequence of the front form. Only in the front form the transition to a moving frame is trivial. In the the instant form the boost operators are non-diagonal and complicated. Note also that these statements hold *if and only if* the interaction in all sectors is identical, *i.e.*

$$U_n(\omega) = U_1(\omega) \ . \tag{55}$$

Is this really true? A word of caution seems to be in place. Actually, *it is not true for any finite* K. The argument is simple: The 'continued fraction' behind the resolvents of resolvents and the Russian puppet structure of the theory becomes interrupted in the last sector. For a finite K there is always a last one, no matter how large K is chosen, and thus the continued fractions in the different sectors do not have the same length and therefore are different. In the *continuum limit*, however, this argument of denumeration does not hold. Thus, for any finite but sufficiently large K the above statement is only 'sufficiently true'.

The resolvents of $\overline{H}_n$, in general, are non-diagonal matrices in Fock space representation. Transforming to the representation in which $\overline{H}_n$ is diagonal, one gets for $n = 3$

$$\begin{aligned} \langle q;\bar{q};g|\overline{G}_3(\omega)|q';\bar{q}';g'\rangle &= \langle q;\bar{q};g|\frac{1}{\omega - \overline{H}_3(\omega)}|q';\bar{q}';g'\rangle \\ &= \sum_{b,s}\langle q;\bar{q};g|\Psi_{b,s}\rangle\langle\Psi_{b,s}| \frac{1}{\omega - \frac{M_b^2+\vec{k}_{g_\perp}^2}{(1-x_g)} - \frac{\vec{k}_{g_\perp}^2}{x_g}} |\Psi_{b,s}\rangle\langle\Psi_{b,s}|q';\bar{q}';g'\rangle \ . \end{aligned} \tag{56}$$

Consider now the resolvent $\overline{G}(\omega)$ as function of ω. It depends, of course, on the value of ω *and on the spectral distribution of the eigenvalues*. Henceforward, as being reasonable for a 'bound state calculation', we shall *restrict to the spectral region where the eigenvalues are sufficiently well separated from each other*. $\overline{G}(\omega)$ will be strongly peaked whenever ω hits one of the true eigenvalues, say $\omega = M_{b'}^2(\omega)$, according to Eq.(24). *At the peak* of this function, however, the following sequence of steps can be performed:

$$\langle q;\bar{q};g|\overline{G}_3(\omega)|q';\bar{q}';g'\rangle = \sum_{b,s}\langle q;\bar{q};g|\Psi_{b,s}\rangle \frac{1}{M_{b'}^2 - \frac{M_b^2+\vec{k}_{g_\perp}^2}{(1-x_g)} - \frac{\vec{k}_{g_\perp}^2}{x_g}} \langle\Psi_{b,s}|q';\bar{q}';g'\rangle \tag{57}$$

$$\simeq \sum_{b,s} \langle q;\bar{q};g|\Psi_{b,s}\rangle \frac{1}{M_{b'}^2 - M_b^2 - \frac{\vec{k}_{g_\perp}^2}{x_g}} \langle \Psi_{b,s}|q';\bar{q}';g'\rangle \tag{58}$$

$$\simeq -\frac{x_g}{\vec{k}_{g_\perp}^2} \sum_{b,s} \langle q;\bar{q};g|\Psi_{b,s}\rangle\langle \Psi_{b,s}|q';\bar{q}';g'\rangle \tag{59}$$

$$= -\frac{x_g}{\vec{k}_{g_\perp}^2} \langle q;\bar{q};g|q';\bar{q}';g'\rangle \ . \tag{60}$$

The first step invokes a *new smallness condition*:

$$x_g \ll \epsilon \leq 1 \qquad \textbf{and} \quad \vec{k}_{g_\perp}^2 \ll \widetilde{\Lambda}^2 \leq M_b^2 \ . \tag{61}$$

It has a completely different origin than the cut-offs Λ_n introduced for Fock-space regularization. The second step, including closure, is not only permitted but also a valid approximation in line with standard many-body technology.

No approximation, however, is involved relating the off-shell mass $\vec{k}_{g_\perp}^2/x_g$ of the gluon to the other particles in $|q;\bar{q};g\rangle$. Denoting the single-particle four-momentum of the gluon, the quark, and the antiquark by k_g,k_q, and $k'_{\bar{q}}$, respectively, only well-known light-cone kinematics is needed to establish that the two four-vectors

$$l_{\bar{q}}^\mu = \left(k_g + k'_{\bar{q}} - k_{\bar{q}}\right)^\mu = \frac{\vec{k}_{g_\perp}^2}{2k_g^+}\,\eta^\mu \quad \text{and} \quad l_q^\mu = \left(k_g + k_q - k'_q\right)^\mu = \frac{\vec{k}_{g_\perp}^2}{2k_g^+}\,\eta^\mu \tag{62}$$

are identical, and proportional to the time-like vector

$$\eta^\mu = (\eta^+, \vec{\eta}_\perp, \eta^-) = (0, \vec{0}_\perp, 2) \ , \tag{63}$$

with $\eta^2 = 0$. The identities

$$\frac{\vec{k}_{g_\perp}^2}{x_g} = (k_g + k_q + k'_{\bar{q}})^2 - (k_q + k_{\bar{q}})^2 = -\frac{1}{x_g}\left(k'_{\bar{q}} - k_{\bar{q}}\right)^2 \tag{64}$$

$$= (k_g + k_q + k'_{\bar{q}})^2 - (k'_q + k'_{\bar{q}})^2 = -\frac{1}{x_g}\left(k_q - k'_q\right)^2 \tag{65}$$

are then obtained straightforwardly.

Some words of caution seem to be in place. (1) The smallness condition requires that $\widetilde{\Lambda}$ is smaller than the lowest bound state. Restraining the transverse momentum of the gluon to be less than the pion mass is not a serious draw-back. One should note that the off-shell mass of the gluon can be large irrespective of how well the smallness condition is fulfilled. (2) One can state with certainty, that the above reduction is inadequate if not false at sufficiently large values of ω, where one might be in the region of 'overlapping resonances' [42]. This will require different technologies and possibly those based on random matrix models [43, 44]. It is there where the concept of a *temperature* will find its way into the bound state problem of gauge field theory.

Finally, the resolvent in the $q\bar{q}\,g$-sector has determined itself to be very simple: *In the solution, the resovents $\overline{G}_n$ are diagonal in Fock-space representation and strictly independent of ω. Instead of having 'resolvents of resolvents' the hierarchy of resolvents is broken. The particles 'in medium' propagate like free particles.*

6 The effective interaction for Gauge Theory

The above considerations are summarized as follows. The effective Hamiltonian

$$H_{\text{eff}} = T + U + U_a \tag{66}$$

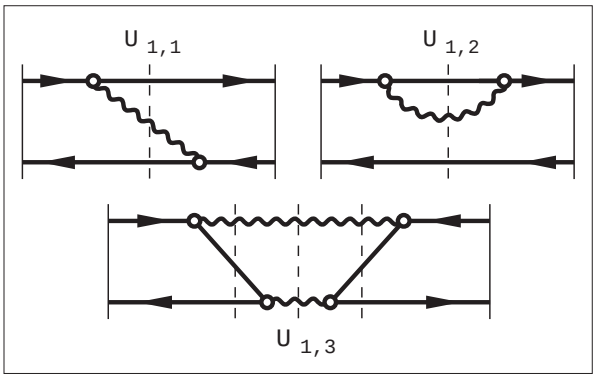

Figure 7: *The full effective interaction in the $q\bar{q}$-space, resumed to all orders in the bare coupling constant. Circles represent the running coupling constant. The one-gluon exchange interaction $U \equiv U_{1,1} + U_{1,2}$ provides the binding. The annihilation interaction $U_a \equiv U_{1,3}$ can be active only if the quarks have the same flavor.*

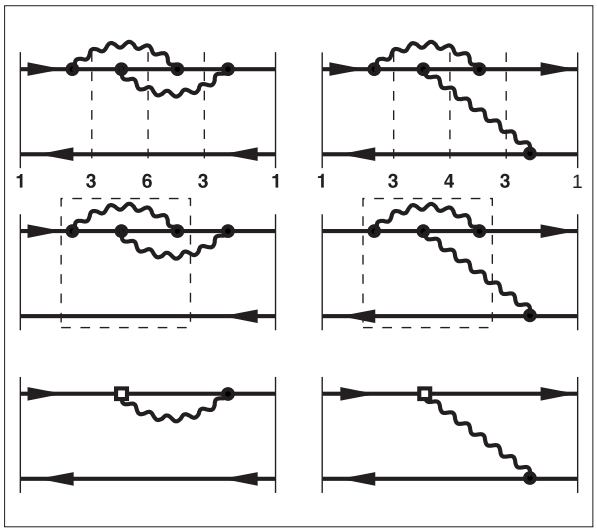

Figure 8: *Two typical graphs, taken from Figure 6, should illustrate how the propagator box (dashed line) contracts into a square around the vertex.*

is supposed to be diagonalized *only in the $q\bar{q}$-space*. The eigenvalue equation $H_{\rm eff}\,|\psi_b\rangle = E_b\,|\psi_b\rangle$ can be understood as the finite dimensional (N_s) matrix equation

$$\sum_{j=1}^{N_s} \langle i|H_{\rm eff}|j\rangle\langle j|\psi_b\rangle = E_b\ \langle i|\psi_b\rangle\ , \qquad \text{for } i = 1, 2, \ldots, N_s. \tag{67}$$

Subject to fixed values of P^+ and $\vec{P}_\perp$, the basis states $|j\rangle$ denumerate all possible Fock states

$$|j\rangle = |q, \bar{q}\rangle = b_q^\dagger d_{\bar{q}}^\dagger |0\rangle, \qquad \text{or} \quad |q, \bar{q}\rangle = |x, \vec{k}_\perp; \lambda_q, \lambda_{\bar{q}}\rangle\ . \tag{68}$$

It often suffices to label an individual Fock state by the momenta of the quark $x \equiv x_q$ and $\vec{k}_\perp \equiv \vec{k}_{q_\perp}$, since the antiquark has $x_{\bar{q}} = 1 - x$ and $\vec{k}_{\bar{q}_\perp} = -\vec{k}_\perp$. The effective Hamiltonian has a kinetic energy T and two kinds of potential energies U. As operators acting in Fock space they are defined by

$$T = \sum_q b_q^\dagger b_q \left(\frac{m^2 + \vec{k}_\perp^{\,2}}{x}\right)_q + \sum_{\bar{q}} d_{\bar{q}}^\dagger d_{\bar{q}} \left(\frac{m^2 + \vec{k}_\perp^{\,2}}{x}\right)_{\bar{q}}\ , \tag{69}$$

$$U = \sum_{q,\bar{q},q',\bar{q}'} b_q^\dagger d_{\bar{q}}^\dagger d_{\bar{q}'} b_{q'}\ \langle q, \bar{q}|\,\widetilde{U}\,|q', \bar{q}'\rangle\ \delta_{f_q, f_{q'}}\ \delta_{f_{\bar{q}}, f_{\bar{q}'}}\ , \tag{70}$$

$$U_a = \sum_{q,\bar{q},q',\bar{q}'} b_q^\dagger d_{\bar{q}}^\dagger d_{\bar{q}'} b_{q'}\ \langle q, \bar{q}|\,\widetilde{U}_a\,|q', \bar{q}'\rangle\ \delta_{f_q, f_{\bar{q}}}\ \delta_{f_{q'}, f_{\bar{q}'}}\ . \tag{71}$$

One distinguishes a flavor-conserving (U) and a flavor-changing effective interaction (U_a). Both of them scatter a quark from state q to state q', and the antiquark from $\bar{q}$ to $\bar{q}'$. They are given diagrammatically in Figure 7, and more formally by

$$U = V\,G_3\,V = V\,R_3^\dagger \overline{G}_3 R_3\,V\ , \qquad \text{and} \tag{72}$$

$$U_a = V\,G_3\,V G_2 V\,G_3\,V = V\,R_3^\dagger \overline{G}_3 R_3\,V G_2 V\,R_3^\dagger \overline{G}_3 R_3\,V\ . \tag{73}$$

Most importantly, the propagator $\overline{G}_3$ (but *not* G_3!) 'in the solution' is *diagonal in Fock space representation*, its numerical value being closely related to the momentum transfer Q of the quarks,

$$\langle q;\bar{q};g|\overline{G}_3|q'';\bar{q}'';g''\rangle = \frac{x_g}{Q^2}\ \langle q;\bar{q};g|q'';\bar{q}'';g''\rangle\ , \qquad \text{with} \quad Q^2 = (k_q - k'_q)^2\ . \tag{74}$$

The operators R had been defined in Eq.(42); here they read

$$R_3 = \frac{1}{\sqrt{1-\overline{G}_3\widetilde{U}_3}}\ . \tag{75}$$

What is their interpretation?

6.1 The Running Coupling Constant

The role of R becomes more obvious when setting $R = 1$ but keeping $R^\dagger$ in Eq.(72),

$$U \simeq V R_3^\dagger \overline{G}_3 V\ . \tag{76}$$

Expanding $R^\dagger$ to first non-trivial order, picking out a particular term, one gets diagrams like in Figure 8, or formally

$$U \simeq V\overline{G}_3 V + \frac{1}{2} V\overline{G}_3 V\overline{G}_6 V\overline{G}_3 V + \dots\ . \tag{77}$$

As mentioned already, a propagator should be represented rather by a box than by a vertical line. This becomes important when the propagator is diagonal, see Eq.(74), *i.e.* when it does not change the momenta of the 'in-' and 'out-states'. As shown in Figure 8, the surrounding box lines can then be contracted over the exchanged gluon. The in- and out-momenta of the R-box are then determined only by the quark single-particle four-momenta k_q and k'_q. Note that these two also determine uniquely the four-momentum of the irradiated gluon. Therefore, in Fock-space representation, the operator R must be a *function of* k_q *and* k'_q alone, and thus only a function of the four-momentum transfer Q as defined in Eq.(74). The *vertex function*

$$\langle k_q|R|k'_q,k_g\rangle = r(k_q,k'_q;\Lambda,m_q,g) = r(Q,\Lambda) \tag{78}$$

depends thus on all variables in the problem, particularly on Q and the cut-offs Λ. As the figure demonstrates, the operator R and its matrix elements *are closely related to the running coupling constant*: both have the same perturbative expansion [45, 46]. But it should be emphasized that perturbative expansions are used here only for the purpose of illustration. The present formalism, particularly Eq.(75), resumes it to all orders in the bare coupling constant, contrary to the familiar expressions gained from perturbation theory [45, 46]. One should mention here the potential danger hidden in the cut-off depence of $r(Q,\Lambda)$. Perturbative estimates yield diverging expressions for ever increasing value of Λ. The problems related to these well-known divergencies will be discussed in future work, see also section 6.3.

6.2 The effective interaction

The actual computation of the vertex function $r(Q,\Lambda)$ as function of all its parameters clearly goes beyond the scope of the present work and must be left to the future, despite its importance. By the same reason, the computation of the annihilation interaction can not be given here. Rather shall we restrict ourselves here to calculate explicitly the flavor-conserving interaction U.

Consider the matrix element $U_{1,1}$ in Figure 7. In this graph, an initial state $|q,\bar{q}\rangle$ state is scattered into a final state $|q',\bar{q}'\rangle$, going through an intermeditate state $|q',\bar{q},g\rangle$. As an adventage of DLCQ, one can introduce these states as to be ortho-normalized and invariant under $SU(N)$:

$$|q,\bar{q}\rangle = \frac{1}{\sqrt{n_c}}\sum_{c=1}^{n_c} b_c^\dagger(k_q,\lambda_q)d_c^\dagger(k_{\bar{q}},\lambda_{\bar{q}})|vac\rangle \ , \tag{79}$$

$$|q',\bar{q}'\rangle = \frac{1}{\sqrt{n_c}}\sum_{c=1}^{n_c} b_c^\dagger(k'_q,\lambda'_q)d_c^\dagger(k'_{\bar{q}},\lambda'_{\bar{q}})|vac\rangle \ , \qquad \text{and} \tag{80}$$

$$|q',\bar{q},g\rangle = \sqrt{\frac{2}{n_c^2-1}}\sum_{c=1}^{n_c}\sum_{c'=1}^{n_c}\sum_{a=1}^{n_c^2-1} T^a_{c,c'} b_c^\dagger(k'_q,\lambda'_q)d_c^\dagger(k_{\bar{q}},\lambda_{\bar{q}})a_a^\dagger(k_g,\lambda_g)|vac\rangle \ . \tag{81}$$

The color matrices $T^a_{c,c'}$ are normalized as usual by $2\mathrm{Tr}(T^aT^b)=\delta_{a,b}$. Since the gluon has a positive value of k_q^+, one necessarily has either

$$k_q^+ > k_q'^+ \qquad \text{or} \qquad k_{\bar{q}}^+ > k_{\bar{q}}'^+ \ . \tag{82}$$

We restrict here to the former. The calculation of the vertex interaction proceeds in two steps. By means of the tables [13], one calculates the vertex matrix elements, separately for emission and absorbtion of the gluon,

$$\langle q,\bar{q}|\,VR^\dagger\,|q',\bar{q},g\rangle = \sqrt{\frac{n_c^2-1}{2n_c}}\,\sqrt{\frac{g^2r^2(Q,\Lambda)}{\Omega\,P^+}}\,\frac{\left[\overline{u}(k_q,\lambda_q)\,\gamma^\mu\epsilon_\mu(k_g,\lambda_g)\,u(k'_q,\lambda'_q)\right]}{\sqrt{x_qx'_qx_g}} \ , \tag{83}$$

$$\langle q',\bar{q},g|\,RV\,|q',\bar{q}'\rangle = -\sqrt{\frac{n_c^2-1}{2n_c}}\,\sqrt{\frac{g^2r^2(Q,\Lambda)}{\Omega\,P^+}}\,\frac{\left[\overline{u}(k_{\bar{q}},\lambda_{\bar{q}})\,\gamma^\nu\epsilon^\star_\nu(k_g,\lambda_g)\,u(k'_{\bar{q}},\lambda'_{\bar{q}})\right]}{\sqrt{x_{\bar{q}}x'_{\bar{q}}x_g}} \ , \tag{84}$$

respectively. Since both the (LC)-Hamiltonian and the Fock states are color neutral, all color algebra has reduced into the overall factor $(n_c^2-1)/2n_c$. According to Eq.(72) one has to sum over all intermediate states. Since the momenta are fixed, only the sum over the two gluon helicities remains, which is done in the usual way:

$$d_{\mu\nu}(k_g)\equiv\sum_{\lambda_g}\epsilon_\mu(k_g,\lambda_g)\,\epsilon^\star_\nu(k_g,\lambda_g) = -g_{\mu\nu}+\frac{k_{g,\mu}\eta_\nu+k_{g,\nu}\eta_\mu}{k_g^\kappa\eta_\kappa} \ . \tag{85}$$

The time-like vector η had been defined in Eq.(63). In Appendix E it is shown how the gauge remnant of the polarization sum cancels exactly against the contribution from the instantaneous interaction. The latter, remember, appears since one works in the light-cone gauge $A^+=0$. The remainder due to $g_{\mu\nu}$ becomes then manifestly gauge invariant:

$$\langle q,\bar{q}|\widetilde{U}|q',\bar{q}'\rangle = \frac{2(2\pi)^3}{\Omega P^+}\,\langle q,\bar{q}|U|q',\bar{q}'\rangle \ , \tag{86}$$

$$\text{with}\quad \langle q,\bar{q}|U|q',\bar{q}'\rangle = -\frac{1}{4\pi^2}\,\frac{\beta(Q,\Lambda)}{Q^2}\,\frac{\langle\lambda_q,\lambda_{\bar{q}}|S(Q)|\lambda'_q,\lambda'_{\bar{q}}\rangle}{\sqrt{x_q(1-x_q)\,x'_q(1-x'_q)}} \ , \tag{87}$$

$$\text{and}\quad \langle\lambda_q,\lambda_{\bar{q}}|S(Q)|\lambda'_q,\lambda'_{\bar{q}}\rangle = \left[\overline{u}(k_q,\lambda_q)\,\gamma^\mu\,u(k'_q,\lambda'_q)\right]\left[\overline{u}(k_{\bar{q}},\lambda_{\bar{q}})\,\gamma_\mu\,u(k'_{\bar{q}},\lambda'_{\bar{q}})\right] . \tag{88}$$

The spinor factor $S(Q)$ collects the familiar and *manifestly Lorentz invariant* current-current interaction, which ultimately will be responsible for the fine and hyperfine structure.

The bare coupling constant g is combined with the vertex function $r(Q,\Lambda)$ into the like-to-be 'running coupling constant' $\beta(Q,\Lambda)$,

$$\beta(Q,\Lambda) = \frac{n_c^2-1}{2n_c}\ \frac{g^2}{4\pi\hbar c}\ r^2(Q,\Lambda)\ . \tag{89}$$

For QCD the gauge group factor $(n_c^2-1)/2n_c$ reduces to 4/3, for QED it has the value 1. It is here where the essential difference of Abelian and non-Abelian gauge theory appears: The coupling constant runs differently. As a consequence, the one is confining and the other one is not. — The graph $U_{1,2}$ in Figure 7 is computed correspondingly.

In the discretized case of the matrix equation, no divergencies can occur because of the regularization. In practical work, however, and by matter of principle, it is more convenient to go to the *continuum limit* $K \to \infty$, simply by replacing sums with integrals. The conversion factor from Eq.(13) cancels against the corresponding factor in Eq.(86), and the *matrix equation* (67) is converted into the *integral equation*

$$M_b^2\langle x,\vec{k}_\perp;\lambda_q,\lambda_{\bar q}|\psi_b\rangle = \left[\frac{m_q+\vec{k}_\perp^{\,2}}{x}+\frac{m_{\bar q}+\vec{k}_\perp^{\,2}}{1-x}\right]\langle x,\vec{k}_\perp;\lambda_q,\lambda_{\bar q}|\psi_b\rangle$$
$$+\frac{1}{4\pi^2}\sum_{\lambda_q',\lambda_{\bar q}'}\int^{\Lambda} dx'd^2\vec{k}_\perp'\ \frac{\beta(Q,\Lambda)}{Q^2}\ \frac{\langle\lambda_q,\lambda_{\bar q}|S(Q)|\lambda_q',\lambda_{\bar q}'\rangle}{\sqrt{x_q(1-x_q)x_q'(1-x_q')}}\left[\langle x,\vec{k}_\perp;\lambda_q,\lambda_{\bar q}|\psi_b\rangle-\langle x',\vec{k}_\perp';\lambda_q',\lambda_{\bar q}'|\psi_b\rangle\right]. \tag{90}$$

The Λ should remind to the fact that the integration over the perpendicular momenta is restricted to a range consistent with Eqs.(14) and (61). Up to the omitted annihilation term, the resulting eigenvalues M_b^2 *must* coincide with the eigenvalues of the full Hamiltonian as shown above. The mass M_b *must be interpreted* as the mass of a physical meson. The corresponding wavefunctions $\langle x,\vec{k}_\perp;\lambda_q,\lambda_{\bar q}|\psi_b\rangle$ give the probability amplitudes for finding in that meson a quark with momentum (fraction) $\vec{k}_\perp\,(x)$ and helicity λ_q. Finally, one should emphasize that the front-form effective Hamiltonian, appearing as the kernel of the integral equation (90), is *manifestly boost invariant*.

6.3 Renormalization Group analysis

The integral equation (90) can be solved for any fixed value of the cut-offs Λ. Therefore, both the wavefunctions and the eigenvalues depend explicitly on it, $M_b = M_b(\Lambda)$.

This is unphysical, since a physical results should not depend on mathematical tricks like regularization. Beyond that it is potentially dangerous since the vertex function diverges as a function of Λ. The way out is, a future renormalization group analysis. One has to require that the solutions do not depend on the cut-off

$$d\,M_b(\Lambda;m,\beta;Q) = 0, \qquad \text{or} \quad \delta_\Lambda M_b\ +\delta_m M_b\ +\delta_\beta M_b = 0\ , \tag{91}$$

at a particular scale set by the momentum transfer Q^2. The renormalization group analysis has thus far been done only for asymptotically large $Q^2 \to \infty$. It is a well established fact, even in light-cone quantization [11, 13, 47, 48], that asymptotically holds $\beta(Q) \longrightarrow \beta_0/\ln(Q^2/\kappa^2)$, with a coefficient β_0 well-known from theory and a mass scale κ which must be determined from experiment. The only difference between the textbooks and the present approach is, that the coupling function $\beta(Q)$ must be calculable down to momentum-transfer zero. The latter is required when one solves the integral equation. Here is the problem, and here we must leave it, since the explicit calculation of $r(Q,\Lambda)$ and the subsequent renormalization of $\beta(Q,\Lambda)$ to yield a $\beta(Q,\kappa)$ clearly goes beyond the scope of the present work. But we have spotted where the problem is.

6.4 Retrieving the full wavefunction

One should emphasize finally that the knowledge of the $q\bar{q}$-space eigenfunction ψ_b is sufficient to retrieve all desired Fock-space components of the total wavefunction Ψ. The key is the upwards recursion relation Eq.(30), *i.e.*

$$\langle n|\Psi\rangle = \sum_{j=1}^{n-1} G_n \langle n|H_n|j\rangle\langle j|\Psi\rangle \ . \tag{92}$$

Obviously, one can express the higher Fock-space components $\langle n|\Psi\rangle$ as functionals of ψ by a finite series of quadratures (or matrix multiplications). One does not have to solve another eigenvalue problem. In order to show this, we ask for the probabilty amplitude to find a $gg(2)$ or a $q\bar{q}\,g(3)$ state in a particular meson b as an example. With $\langle 1|\Psi\rangle = \langle q\bar{q}|\psi_b\rangle$ the first two relevant equations of (92) are

$$\langle 2|\Psi\rangle = G_2\langle 2|H_2|1\rangle\langle 1|\Psi\rangle \ , \qquad \text{and} \tag{93}$$

$$\langle 3|\Psi\rangle = G_3\langle 3|H_3|1\rangle\langle 1|\Psi\rangle + G_3\langle 3|H_3|2\rangle\langle 2|\Psi\rangle \ . \tag{94}$$

Note that $\langle 2|\Psi\rangle$ is expressed already in terms of $\langle 1|\Psi\rangle$. The sector Hamiltonians H_n have been dealt with in sections 4 and 5. They can be expressed by chains with the bare interaction V, particularly $H_2 = T + V + VG_3V + VG_5V$ and $H_3 = T + V + VG_4V + VG_6V + VG_6VG_5VG_6V$. With the abbreviation $V_{ij} \equiv \langle i|V|j\rangle$ and the 'selection rules' of Figure 2 one gets $\langle 2|H_2|1\rangle = V_{23}G_3V_{21}$, $\langle 3|H_3|1\rangle = V_{31}$, $\langle 3|H_3|2\rangle = V_{32}$, and therefore

$$\langle 2|\Psi\rangle = G_2V_{23}G_3V_{21}\langle 1|\Psi\rangle, \qquad \text{and} \tag{95}$$

$$\langle 3|\Psi\rangle = G_3V_{31}\langle 1|\Psi\rangle + G_3V_{32}G_2V_{23}G_3V_{21}\langle 1|\Psi\rangle \ . \tag{96}$$

One should emphasize again that these expressions are exact to all orders in the coupling constant. The propagators have to be treated like exposed in section 5. They include the running coupling constant and in the solution are independent of ω. Obviously, the procedure is straightforward, well-defined, and actually simple.

7 Summary and Perspectives

In the present work, one adopts the point of view that most, if not all, properties of a Lagrangian gauge field theory are contained in the canonical front-form Hamiltonian, which is calculated in the light-cone gauge omitting the zero modes. Periodic boundary conditions allow to construct explicitly the Hamiltonian matrix for fixed harmonic resolution. Rows and columns of this matrix refer to all possible momentum states of 2, 3, or more particles. All variables are well defined, finite and denumerable: The total longitudinal momentum and the harmonic resolution are finite, the number of states and the number of sectors are finite, and last but not least every single matrix element of the Hamiltonian is finite. One is confronted with the diagonalization of a finite block matrix and applies the theory of effective interactions in conjunction with the method of iterated resolvents. As shown, one can map the large Hamiltonian matrix without smallness assumption onto a matrix problem with much smaller dimensions, to the problem of diagonalizing the effective Hamiltonian in the $q\bar{q}$-space. It is shown why *these two matrices have the same eigenvalues.* At the end, the periodic boundary conditions are relaxed by the limiting process of going over to the continuum limit.

The diagrammatic representation of the effective interaction as given in Figure 7 looks like second order diagrams of perturbation theory. But despite this, they are far from being that: due

to the vertex function (which after renormalization is related to the running coupling constant), they represent a resummation of pertubative graphs to all orders in the bare coupling constant. The effective interaction U is computed explicitly in section 6. It is our understanding that $U + U_a$ represents an exact mapping of the full many-body Hamiltonian onto the $q\bar{q}$ space. Solving for the eigenfunctions in this space one can retrieve all other many-body amplitudes of the wavefunction in a self-consistent way, as shown in section 6.

To arrive at this simple result it is crucial to include arbitrarily many gluons. Only then, as argued in section 5, the Russian puppet structure of 'resolvents within resolvents' can be used as an argument why the effective interaction is the same in all hierarchies. It is precisely this aspect of self-similarity in a gauge theory which ultimately allows for the 'breaking of the hierarchy': In the solution, the particles propagate like free particles and all many-body aspects reside in the vertex coupling function. One can overstress the point for QED by stating that the generation of the simple Coulomb potential requires infinitely many photons. Finally, one should emphasize that the present approach needs no 'convergence-improving' external potential as in [19], which once introduced is so difficult to get rid-off. The average potential generates itself, in the solution.

The present work claims to connect a Lagrangian gauge field theory with the eigenvalues and eigenfunctions of a bound state equation. We like to emphasize that all steps can be (dis-)verified numerically in a well defined manner. One can start with a sufficiently large DLCQ-Hamiltonian matrix, as large as the computer can digest. The reduction to the effective Hamiltonian can then be done by successive matrix inversions and multiplications as described in Sections 3 and 4. The prediction is that the lower eigenvalues depend only weakly on the starting point energy. In addition, one can (dis-)verify numerically *a posteriori* how well the succesive approximations from Eqs. (57) to (58) to (59) are satisfied in practice.

Important as the present work might be, it only can be the first step. The resulting effective potential depends on several formal and unphysical parameters, among them the harmonic resolution K and the transversal length $L_\perp$ induced both by the periodic boundary conditions, the cut-off scale Λ regulating the transversal momenta, and finally the smallness parameters ϵ and $\widetilde{\Lambda}$. The resolution and the length disappear when going to the continuum limit. But the dependence on Λ, ϵ and $\widetilde{\Lambda}$ remains. The second, and perhaps even more important step, must therefore be to remove them by a renormalization group analysis [45, 46]. This has not been done, yet. The present work thus culminates and ends at a pre-renormalization stage. The merit of the present work is to pinpoint the object of renormalization, namely the vertex function which is given here for the first time in a non-perturbative formulation to all orders in the coupling constant.

But even before a future renormalization group analysis the present formalism is useful and has some rather nice aspects: Even without knowing the explicit structure of the running coupling constant in the infinite momentum frame one can do some educated guess work. For example, using Richardson's version [49] of the running coupling constant one can establish confinement in a parameter-free fashion. One can approximately, but analytically, calculate the heavy meson masses based on the parametric variation of a trial wave function [50]. An explicit, but numerical, solution of the same problem is currently being attempted [51]. Last but not least one can choose the smallness parameters $\widetilde{\Lambda}$ so small that no transversal momenta survive at all. One then ends up with a 'collinear model' [53] similar to the dimensionally reduced models solved thus far [24, 36, 37], resulting in stupendous analytical properties of the light mesons [52]. These features make it worth to communicate the present work even prior to a renormalizaton group analysis.

Acknowledgement. I am grateful to Uwe Trittmann and Rolf Bayer, who have devoted much time to help me in the early phases of this work. In particular, I thank Uwe for preparing Figure 9 for me, among many others not shown. I thank my friends Profs. Steve Pinsky from OSU and Stan Brodsky from SLAC for their patience and help to improve my never ending illiteracy on field theory off and on the light cone.

References

[1] W. Lucha, F.F. Schöberl, and D. Gromes, Phys. Rept. **200**, 127 (1991); and references therein.

[2] P.B. Mackenzie, *Status of Lattice QCD,* In: Ithaka 1993, Proceedings of 'Lepton and Photon Interactions', p.634; `hep-ph 9311242;` and references therein.

[3] D. Weingarten, Nucl. Phys. (Proc. Supp.) **B34**, 29 (1994); and references therein.

[4] C.T.H. Davies, A.J. Lindsay, K. Hornbostel, G.P. Lepage, J. Shigemitsu, and J. Sloan, *B_c and Υ Spectra from Lattice NRQCD*, `hep-lat/9510052 -- Oct 1995`.

[5] S. Godfroy and N. Isgur, Phys.Rev. **32D**, 189 (1985).

[6] See for example: Yu.L. Dokshitzer, V.A. Khoze, A.H. Mueller and S.I. Troyan, *Basics of perturbative QCD*, (Editions Frontières, Gif-sur-Yvette, 1991).

[7] M. Neubert, Phys. Lett. **C245** (1994) 259; and references therein.

[8] Es.J. Eichten and Ch. Quigg, *Mesons with Beauty and Charm*, `hep-lat/9402210 -- Feb 1994`.

[9] P.A.M. Dirac, Rev. Mod. Phys. **21**, 392 (1949).

[10] G.P. Lepage and S.J. Brodsky, Phys.Rev. **D22**, 2157 (1980).

[11] G.P. Lepage, S.J. Brodsky, T. Huang, P.B. Mackenzie, *Proceedings of the Banff Summer Institute*, 1981.

[12] S.J. Brodsky and G.P. Lepage, in *Perturbative Quantum Chromodynamics,* A. H. Mueller, Ed. (World Scientific, Singapore, 1989)

[13] S.J. Brodsky and H.C. Pauli, in *Recent Aspects of Quantum Fields,* H. Mitter and H. Gausterer, Eds., Lecture Notes in Physics, Vol 396, (Springer, Heidelberg, 1991); and references therein.

[14] *Theory of Hadrons and Light-front QCD,* S.D. Glazek, Ed., (World Scientific Publishing Co., Singapore, 1995).

[15] H.C. Pauli and S.J. Brodsky, Phys.Rev. **D32**, 1993 (1985).

[16] H.C. Pauli and S.J. Brodsky, Phys.Rev. **D32**, 2001 (1985).

[17] T. Eller, H.C. Pauli and S.J. Brodsky, Phys.Rev. **D35**, 1493 (1987).

[18] K. Wilson, in *Lattice '89*, R. Petronzio, *Ed.*, Nucl.Phys. (Proc. Suppl.) **B17**, (1989).

[19] K.G. Wilson, T. Walhout, A. Harindranath, W.M. Zhang, R.J. Perry, and S.D. Glazek, Phys. Rev. **D49**, 6720 (1994); and references therein.

[20] T. Heinzl, S. Krusche, S. Simburger, and E. Werner, Z. Phys. **C56**, 415 (1992).

[21] B. Vandesande and S.S. Pinsky, Phys. Rev. **D46**, 5479 (1992).

[22] S.S. Pinsky, and B. Vandesande, Phys. Rev. **D49**, 2001 (1994).

[23] A.C. Kalloniatis, and H.C. Pauli, Z.Phys. **C63**, 161 (1994) .

[24] H.C. Pauli, A.C. Kalloniatis, and S.S. Pinsky, Phys.Rev. **D52**, 1176 (1995).

[25] A.C. Tang, S.J. Brodsky, and H.C. Pauli, Phys.Rev. **D44**, 1842 (1991).

[26] M. Krautgärtner, H.C. Pauli and F. Wölz, Phys.Rev. **D45**, 3755 (1992).

[27] M. Kalu V za and H.C. Pauli, Phys. Rev. **D45**, 2968 (1992).

[28] F. Wölz, PhD Thesis, U. Heidelberg (1995).

[29] I. Tamm, J.Phys. (USSR) **9**, 449 (1945).

[30] S.M. Dancoff, Phys.Rev. **78**, 382 (1950).

[31] G.T. Bodwin and D.R. Yennie, Phys.Lett. **43C**, 267 (1978).

[32] G.T. Bodwin, D.R. Yennie, and M. Gregorio, Rev.Mod.Phys. **57**, 723 (1985).

[33] J.R. Sapirstein, E.A. Terray, and D.R. Yennie, Phys.Rev. **D29**, 2990 (1984).

[34] W.E. Caswell and G.P. Lepage, Phys.Rev. **A18**, 810 (1978).

[35] P.M. Morse and H. Feshbach, *Methods in Theoretical Physics*, 2 Vols, Mc Graw-Hill, New York, N.Y., 1953.

[36] H.C. Pauli, and R. Bayer, Phys.Rev. **D53**, 939 (1996).

[37] B. van de Sande, and M. Burkardt, Phys.Rev. **D53**, 4628 (1996).

[38] H.C. Pauli, Nucl.Phys. **A396**, 413 (1981).

[39] D.C. Zheng, J.P. Vary, and B.R.Barret, Nucl.Phys. **A560**, 211 (1993).

[40] H.C. Pauli, Z.Phys. **A319**, 303 (1984).

[41] H.C. Pauli, in *Quantum Field Theoretical Aspects of High Energy Physics,* B. Geyer and E.M. Ilgenfritz, Eds., (Zentrum Höhere Studien, Leipzig, 1993); also available as preprint MPIH-V24-1993, Heidelberg, Oct 1993.

[42] J.J.M. Verbaarschot, H.A. Weidenmüller, and M. Zirnbauer, Phys.Lett. **C129**, 367 (1985).

[43] J.J.M. Verbaarschot, Phys.Rev.Lett. **72**, 2531 (1994).

[44] T. Wettig, A. Schäfer, and H.A. Weidenmüller, Phys.Lett. **B367**, 28 (1996).

[45] D. Gross and F. Wilczek, Phys.Rev.Lett. **26**, 1343 (1973).

[46] H.D. Politzer, Phys.Rev.Lett. **26**, 1346 (1973).

[47] Ch. Thorn, Phys.Rev. **D19**, 639 (1979).

[48] R.J. Perry, A. Harindranath, and W.M. Zhang, Phys.Lett. **B300**, 8 (1993).

[49] J.L. Richardson, Phys.Lett. **82B**, 272 (1979).

[50] H.C. Pauli and J. Merkel, Heidelberg preprint MPIH-V45-1995, submitted to Phys.Rev. **D** (1996).

[51] U. Trittmann, and H.C. Pauli, in preparation, 1996.

[52] R. Bayer and H.C. Pauli, to be submitted to Phys.Rev. **D** (1996).

[53] K. Demeterfi, I.R. Klebanov, and G. Bhanot, Nucl. Phys. **B418**, 15 (1994).

A The 4×4 Block Matrix as a Paradigm

The considerations in section 4 can be substantiated with an explicit example. The rows and columns of any finite dimensional matrix can be grouped into four blocks. The block matrix has then the following shape:

$$\begin{pmatrix} \langle 1|H|1\rangle & \langle 1|H|2\rangle & \langle 1|H|3\rangle & \langle 1|H|4\rangle \\ \langle 2|H|1\rangle & \langle 2|H|2\rangle & \langle 2|H|3\rangle & \langle 2|H|4\rangle \\ \langle 3|H|1\rangle & \langle 3|H|2\rangle & \langle 3|H|3\rangle & \langle 3|H|4\rangle \\ \langle 4|H|1\rangle & \langle 4|H|2\rangle & \langle 4|H|3\rangle & \langle 4|H|4\rangle \end{pmatrix} . \tag{97}$$

The reduction from the 4×4 to the 3×3 matrix is easy: Since $H_4 \equiv H$, one replaces all bare block matrix elements in the 3×3 matrix by $\langle i|H_3|j\rangle$, with

$$H_3 = H + HG_4H \ . \tag{98}$$

Next, reduce the matrix of block matrix dimension 3 to the one of block matrix dimension 2, by $H_2 = H_3 + H_3G_3H_3$. Inserting H_3 from Eq.(98), one gets

$$H_2 = (H + HG_4H) + (H + HG_4H)G_3(H + HG_4H) \ . \tag{99}$$

Performing reduction and substitution once more one arrives at

$$\begin{aligned} H_1 \ = \ & \Big((H + HG_4H) + (H + HG_4H)G_3(H + HG_4H)\Big)G_2 \\ & \Big((H + HG_4H) + (H + HG_4H)G_3(H + HG_4H)\Big) \ . \end{aligned} \tag{100}$$

One has thus expressed the matrix elements of the effective interaction in sector 1 in terms of the bare interaction H and the resolvents G_2, G_3, and G_4, which in turn are given by the effective interactions H_2, H_3 and H_4, respectively, *i.e.*

$$G_2 = |2\rangle \, \frac{1}{\omega - H_2} \, \langle 2| \ , \quad G_3 = |3\rangle \, \frac{1}{\omega - H_3} \, \langle 3| \ , \quad G_4 = |4\rangle \, \frac{1}{\omega - H} \, \langle 4| \ . \tag{101}$$

Note that all operations are well defined matrix multiplications and inversions. The *bare interactions* H alternate with the resolvents of *effective interactions* H_n to build up *strictly finite chains*. The longest chain in Eq.(100) has 5 propagators: $HG_4HG_3HG_2HG_3HG_4H$. This is in stark contrast to the infinite chains of perturbative series.

B Continued Fractions in Iterated Resolvents

The structure of the chains in the Method of Iterated Resolvents depends quite strongly on the block matrix structure of the matrices considered, as is obvious from Eq.(100) in Appendix A. For to show that explicitly, the example of a matrix with a tridiagonal block structure is choosen, *i.e.*

$$H_B = \begin{pmatrix} H_{11} & H_{12} & . & . \\ H_{21} & H_{22} & H_{23} & . \\ . & H_{32} & H_{33} & H_{34} \\ . & . & H_{43} & H_{44} \end{pmatrix} \ , \qquad \textbf{or} \quad \widetilde{H}_B = \begin{pmatrix} 0 & 1 & . & . \\ 1 & 2 & 3 & . \\ . & 3 & 4 & 5 \\ . & . & 5 & 6 \end{pmatrix} \ , \tag{102}$$

with dots representing zero matrices (H_B) or straight zeros ($\widetilde{H}_B$). Applying the same procedure as in Appendix A, one notes that many of the long chains vanish since for example $G_2HG_4 \equiv G_2 \, H_{24} \, G_4 = 0$. The effective interactions, as given in Eq.(100) for the general 4×4 block matrix,

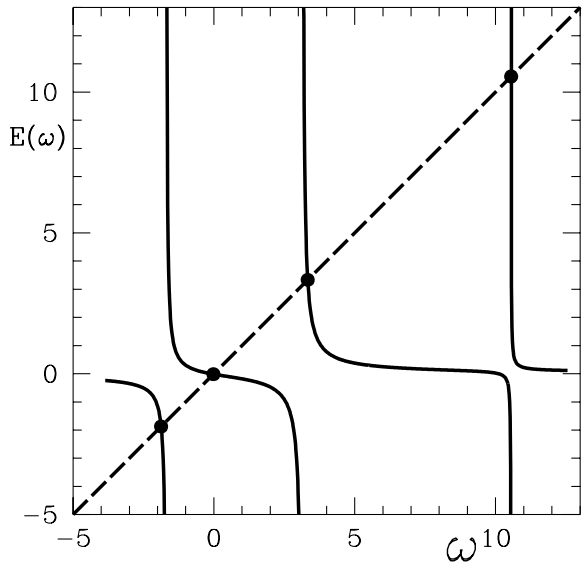

Figure 9: *The energy function $E(\omega)$ for the matrix H_B is plotted versus ω. The solutions of $E(\omega) = \omega$ agree with the four exact eigenvalues -1.87208, -0,01518, 3.33343, and 10.5538.*

simplify strongly. Here, one gets consecutively $H_3 = H + HG_4H$, $H_2 = H + HG_3H$ and $H_1 = H + HG_2H$. The effective Hamiltonian in the 1-space therefore has the structure of a continued fraction:

$$\langle 1|H_1|1\rangle = H_{11} + H_{12}\cfrac{1}{\omega - H_{22} - H_{23}\cfrac{1}{\omega - H_{33} - H_{34}\cfrac{1}{\omega - H_{44}}H_{43}}H_{32}}H_{21} \ . \tag{103}$$

One can test the method of iterated resolvents in an almost trivial way: Assume that each of the blocks in Eq.(102) has dimension 1. The matrix is thus a usual 4×4-matrix. The inverse of a 1×1 'matrix' is trivial. The 'effective Hamiltonian' is also a 1×1 'matrix' identical with the energy function $E(\omega)$. For the matrix $\widetilde{H}_B$ in Eq.(102) one gets simply

$$E(\omega) = \cfrac{1 \cdot 1}{\omega - 2 - \cfrac{3 \cdot 3}{\omega - 4 - \cfrac{5 \cdot 5}{\omega - 6}}} \quad . \tag{104}$$

As displayed in Figure 9, the solutions of the fixpoint equation $E(\omega) = \omega$ agree with the four eigenvalues to within computer accuracy. Note that a form like Eq.(103) or (104) could possibly be useful to diagonalize a tridiagonal matrix of arbitraly large but finite dimension.

C The Chains of the Effective Interaction

The example in Appendix A suggests that the effective interaction wants to develop finite chains of bare Hamiltonian blocks $\langle i|H|j\rangle$ alternating with resolvents of sector Hamiltonians H_n. This can be cast into a systematic procedure, as follows. Sequential application of the recursion relation Eq.(31) allows to derive the useful relation

$$H_n = H + \sum_{m=n+1}^{N} H_m G_m H_m \ . \tag{105}$$

Table 1: *All chains of the effective interaction in the $q\bar{q}$-space H_1 with one, two and three propagators G_i which are associated with the QCD matrix in Figure 1 are enumerated. The square brackets for $H^{(3)}$ refer to the three different sums in the defining Eq.(114).*

#	$H_1^{(1)}$ and $H_1^{(2)}$	#	$H_1^{(3)}[l_3,l_2,l_1]$	#	$H_1^{(3)}[l_3,l_1,l_2]$	#	$H_1^{(3)}[l_3,n_1,r_2]$
1	SG_2S	10	$FG_4VG_3VG_2S$	15	$VG_3SG_5VG_2S$	25	$VG_3VG_2VG_3V$
2	VG_3V	11	$FG_6VG_3VG_2S$	16	$VG_3VG_6FG_2S$	26	$FG_4VG_3VG_4F$
3	FG_4F	12	$FG_6SG_4VG_3V$	17	$FG_4SG_6VG_3V$	27	$FG_6FG_2FG_6F$
4	FG_6F	13	$FG_6VG_5VG_2S$	18	$FG_4SG_6FG_2S$	28	$FG_6VG_3VG_6F$
5	VG_3VG_2S	14	$FG_6VG_5SG_3V$	19	$FG_4VG_7FG_3V$	29	$FG_6SG_4SG_6F$
6	FG_4VG_3V			20	$FG_6VG_7VG_4F$	30	$FG_6VG_5VG_6F$
7	FG_6FG_2S			21	$FG_6VG_7FG_3V$	31	$FG_6FG_2VG_3V$
8	FG_6VG_3V			22	$FG_6SG_9FG_2S$	32	$FG_6VG_3VG_4F$
9	FG_6SG_4F			23	$FG_6VG_{10}FG_3V$		
				24	$FG_6FG_{11}FG_4F$		

To prove this, one writes down $H_1 = H_2 + H_2G_2H_2$ and $H_2 = H_3 + H_3G_3H_3$ and combines them to get $H_1 = H_3 + H_2G_2H_2 + H_3G_3H_3$. This is Eq.(105) for N=3. The general case is proven by induction. Eq.(105) relates the effective interaction in sector n to the bare Hamiltonian H and virtual scatterings into the higher sectors $m > n$. This only *upward scattering* has important consequences for the structure of the chains. How can one classify them? The *number of propagators in a chain* turns out to be a more useful criterium for that than, for example, the order of the coupling constant. If a chain has 3 propagators, it will contribute to $H^{(3)}$. The bare interaction has no propagator and thus is the 'chain' $H^{(0)} = H$. The effective interaction is the sum of all possible chains:

$$H_n = H_n^{(0)} + H_n^{(1)} + H_n^{(2)} + H_n^{(3)} + H_n^{(4)} + H_n^{(5)} + \cdots \ . \tag{106}$$

The expansion is finite for any finite dimensional block matrix. After its insertion into Eq.(105) one reads off *upward recursion relations* with the general term

$$H_n^{(k+1)} = \sum_{l>n} \left(H_l^{(0)} G_l H_l^{(k)} + H_l^{(1)} G_l H_l^{(k-1)} + \cdots + H_l^{(k-1)} G_l H_l^{(1)} + H_l^{(k)} G_l H_l^{(0)} \right) , \tag{107}$$

or explicitly for the first four of them

$$H_n^{(1)} = \sum_{l>n} H_l^{(0)} G_l H_l^{(0)} \quad , \tag{108}$$

$$H_n^{(2)} = \sum_{l>n} \left(H_l^{(0)} G_l H_l^{(1)} + H_l^{(1)} G_l H_l^{(0)} \right) , \tag{109}$$

$$H_n^{(3)} = \sum_{l>n} \left(H_l^{(0)} G_l H_l^{(2)} + H_l^{(1)} G_l H_l^{(1)} + H_l^{(2)} G_l H_l^{(0)} \right) , \tag{110}$$

$$H_n^{(4)} = \sum_{l>n} \left(H_l^{(0)} G_l H_l^{(3)} + H_l^{(1)} G_l H_l^{(2)} + H_l^{(2)} G_l H_l^{(1)} + H_l^{(3)} G_l H_l^{(0)} \right) . \tag{111}$$

For convenience, the chains up to order 4 are tabulated explicitly:

$$H_n^{(1)} = \sum_{l_1>n} H G_{l_1} H \quad , \tag{112}$$

$$H_n^{(2)} = \sum_{l_2>l_1>n} \Big(HG_{l_2}HG_{l_1}H + HG_{l_1}HG_{l_2}H \Big) , \tag{113}$$

$$\begin{aligned} H_n^{(3)} &= \sum_{l_3>l_2>l_1>n} \Big(\; HG_{l_3}HG_{l_2}HG_{l_1}H + HG_{l_1}HG_{l_2}HG_{l_3}H + \\ &\qquad\qquad HG_{l_3}HG_{l_1}HG_{l_2}H + HG_{l_2}HG_{l_1}HG_{l_3}H \; \Big) \\ &+ \sum_{\substack{l_3>n_1>n \\ r_2>n_1>n}} \Big(\; HG_{l_3}HG_{n_1}HG_{r_2}H \; \Big) , \end{aligned} \tag{114}$$

$$\begin{aligned} H_n^{(4)} &= \sum_{l_4>l_3>l_2>l_1>n} \Big(\; HG_{l_4}HG_{l_3}HG_{l_2}HG_{l_1}H + HG_{l_1}HG_{l_2}HG_{l_3}HG_{l_4}H + \\ &\qquad HG_{l_4}HG_{l_1}HG_{l_2}HG_{l_3}H + HG_{l_2}HG_{l_1}HG_{l_3}HG_{l_4}H + \\ &\qquad HG_{l_4}HG_{l_3}HG_{l_1}HG_{l_2}H + HG_{l_3}HG_{l_2}HG_{l_1}HG_{l_4}H + \\ &\qquad HG_{l_4}HG_{l_2}HG_{l_1}HG_{l_3}H + HG_{l_3}HG_{l_1}HG_{l_2}HG_{l_4}H \; \Big) \\ &+ \sum_{\substack{l_4>l_3>l_2>n \\ l_4>l_3>r_1>n}} \Big(\; HG_{l_4}HG_{l_2}HG_{l_3}HG_{r_1}H + HG_{r_1}HG_{l_3}HG_{l_2}HG_{l_4}H \; \Big) \\ &+ \sum_{\substack{l_4>l_3>n \\ l_4>r_2>r_1>n}} \Big(\; HG_{l_3}HG_{l_4}HG_{r_1}HG_{r_2}H + HG_{r_2}HG_{r_1}HG_{l_4}HG_{l_3}H + \\ &\qquad HG_{l_3}HG_{l_4}HG_{r_2}HG_{r_1}H + HG_{r_1}HG_{r_2}HG_{l_4}HG_{l_3}H \; \Big) . \end{aligned} \tag{115}$$

Table 1 enumerates all chains up to order 3 for the full QCD-block-matrix as displayed in Figure 1. For convenience, the type of interaction in the block matrix is accounted for by V, F, and S, refering to vertex-, fork-, and seagull-interactions, respectively.

D The Gauge Trick

The present work has been started keeping track explicitly of the gauge remnants, the seagull and the fork interactions S and F. With the work progressing it was realized that the formal manipulations can be substantially simplified when one includes only the vertex interactions combined with the gauge trick. Rather than formally, the argument is lead here diagrammatically, by way of example in Figure 10 and its caption. Very instructively, one misses there a chain of order 1 which shows up in Table 1, particularly FG_6F. It is found when analyzing the series in Eq.(41) term by term, some of which being displayed diagrammatically in Figure 6. Consider the graph labelled (36b) in the Figure, standing for the chain $V\overline{G}_3V\,G_6\,V\overline{G}_3V$. Now, interprete the two outer gluon lines as instantaneous and write down the corresponding chain: it is the missing FG_6F! The literally hundreds of graphs analyzed diagrammatically in preparing this work, cannot be discussed here in detail, of course. Suffice it to state that *all chains with instantaneous interactions as enumerated in Table 1 have been identified explicitly as the instantaneous partners of dynamical chains like* $VGVGV\ldots GVGVGV$. This should be sufficient evidence for the 'gauge trick ' applied in this work.

E The cancellation of the gauge remnants

Substituting the η-dependent terms of the spinor sum, Eq.(85), into the effective interaction yields straightforwardly

$$\sum_{\lambda_g} \langle q,\bar{q}|\, V R^\dagger \,|q',\bar{q},g\rangle\langle q',\bar{q},g|\, RV \,|q',\bar{q}'\rangle_\eta = -\frac{n_c^2-1}{2n_c}\,\frac{g^2 r^2(Q,\Lambda)}{\Omega\,P^+}\,\frac{(P^+)^2}{x_g k_g^+}\,\times$$

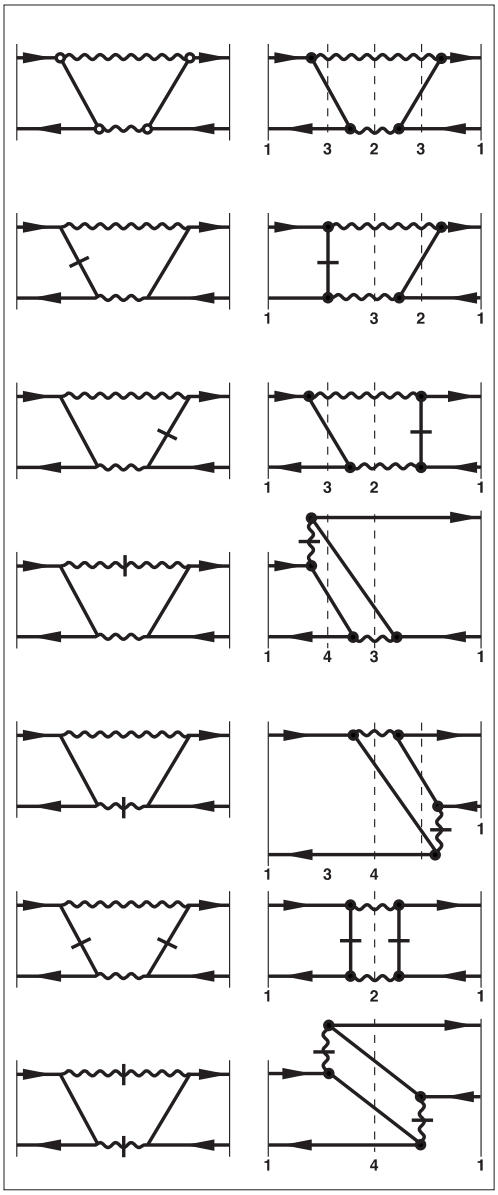

Figure 10: *The annihilation interaction with all instantaneous lines explicitly inserted. The annihilation graph of the effective interaction is displayed in the upper left of the figure. It represents the following three-step procedure: (1) A line in between two interaction points is called a 'physical' line representing the exchange of a physical particle; (2) Every physical line is the sum of a 'dynamical' and an ' instantaneous' line; (3) Two instantaneous lines cannot be connected at a vertex. Drawing all possible diagrams with* $0, 1, 2, \ldots$ *instantaneous lines like in the left of the figure in the convention of Tang [25], one obtains seven gaphs. On the right, the same seven diagrams are drawn in the convention of Brodsky[13]. One can read off there the chains of different order, particularly* SG_2S, FG_4F, VG_3VG_2S, VG_4VG_3F, *and* $VG_3VG_2VG_3V$. *When analyzed in the same way, the gluon exchange graph* $U_{1,1}$ *in Figure 3 provides one with the chain of order zero (*S*) and with* VG_3V. *All of them appear also in Table 1. But one misses a chain of order 1 which appears in the Table, i.e.* FG_6F. *Where is it, and where are the other chains of higher order? — See the discussion in the text.*

$$\times\Big\{\frac{\Big[\overline{u}(q)\gamma_\mu k_g^\mu u(q')\Big]}{P^+\sqrt{x_q x'_q}}\frac{[\overline{u}(\bar{q})\gamma_\nu\eta^\nu u(\bar{q}')]}{P^+\sqrt{x_{\bar{q}}x'_{\bar{q}}}} \quad + \quad \frac{[\overline{u}(q)\gamma_\mu\eta^\mu u(q')]}{P^+\sqrt{x_q x'_q}}\frac{\Big[\overline{u}(\bar{q})\gamma_\nu k_g^\nu u(\bar{q}')\Big]}{P^+\sqrt{x_{\bar{q}}x'_{\bar{q}}}}\Big\}\,. \tag{116}$$

The well-known property of the Dirac spinors

$$(k_q-k'_q)^\mu\left[\overline{u}(k_q,\lambda_q)\,\gamma_\mu\,u(k'_q,\lambda'_q)\right]=0 \tag{117}$$

can be used for constructing the time-like null vectors derived in section 5, *i.e.*

$$l_{\bar{q}}^\mu=\Big(k_g+k'_{\bar{q}}-k_{\bar{q}}\Big)^\mu=\frac{\vec{k}_{g_\perp}^{\,2}}{2k_g^+}\,\eta^\mu \quad\text{and}\quad l_q^\mu=\Big(k_g+k_q-k'_q\Big)^\mu=\frac{\vec{k}_{g_\perp}^{\,2}}{2k_g^+}\,\eta^\mu\,. \tag{118}$$

Together with the resolvent $\overline{G}_3=-x_g/\vec{k}_{g_\perp}^{\,2}$ one gets most directly

$$\begin{aligned}&\sum_{\lambda_g}\langle q,\bar{q}|\,VR^\dagger\,|q',\bar{q},g\rangle\overline{G}_3\langle q',\bar{q},g|\,RV\,|q',\bar{q}'\rangle_\eta=\\&=\frac{n_c^2-1}{2n_c}\,\frac{g^2r^2(Q,\Lambda)}{\Omega\,P^+}\,\frac{1}{x_g^2}\,\frac{[\overline{u}(q)\gamma^+u(q')]}{P^+\sqrt{x_q x'_q}}\frac{[\overline{u}(\bar{q})\gamma^+u(\bar{q}')]}{P^+\sqrt{x_{\bar{q}}x'_{\bar{q}}}}\,.\end{aligned} \tag{119}$$

Compare this with the seagull interaction evaluated directly by means of the tables [13]

$$\langle q,\bar{q}|\,R^\dagger SR\,|q',\bar{q}'\rangle=-\frac{n_c^2-1}{2n_c}\,\frac{g^2r^2(Q,\Lambda)}{\Omega\,P^+}\,\frac{\Big[\overline{u}(k_q,\lambda_q)\gamma^+u(k'_q,\lambda'_q)\Big]}{(x_q-x'_q)^2\;P^+\sqrt{x_q x'_q}}\frac{\Big[\overline{u}(k_{\bar{q}},\lambda_{\bar{q}})\gamma^+u(k'_{\bar{q}},\lambda'_{\bar{q}})\Big]}{P^+\sqrt{x_{\bar{q}}x'_{\bar{q}}}} \tag{120}$$

to conclude that *all gauge artefacts cancel each other precisely.*